



**Advanced Multicomponent
Seismic Software**

**Analysis of seismic data recorded in October 2025
by network C8 (stations SV1S-SV5S)
at Aquistore test site**

Report AQ-2025-10-IM

December 23, 2025

Igor Morozov

igor.morozov@usask.ca

Contents

1. Station performance.....	3
Data recovery.....	3
2. Data quality.....	7
3. Processing procedure and parameters.....	9
4. Seismic event detection.....	10
Automatic detections.....	10
Event bulletins.....	11
Teleseismic events (class 1).....	12
Regional events (class 2).....	15
Local events (classes 3 and 4).....	15
Possible mine blasts at the Estevan mine (class 3a).....	15
Events related to mining operations (class 3b).....	19
Events in array proximity (classes 4a and 4b).....	24
5. SEGY files.....	26
6. Conclusions and recommendations.....	26

1. Station performance

Station performance for October 2025 is summarized in Figure 1, and state-of-health data are shown in Figure 2. Although not visible from these Figures, note two significant issues with station performance:

- Poor data quality from station SV3S due to a failed sensor or sensor cable. The cable was replaced on around October 20, after which the the station started working correctly.
- Poor data quality from channel SV5S.HHE, also likely due to a bad cable. This issue has been present for over a year.

Data recovery

Data recovery from all channels was nearly 100% (Figure 1). Network communication lapsed on October 28-31 but the data were retrieved afterwards.

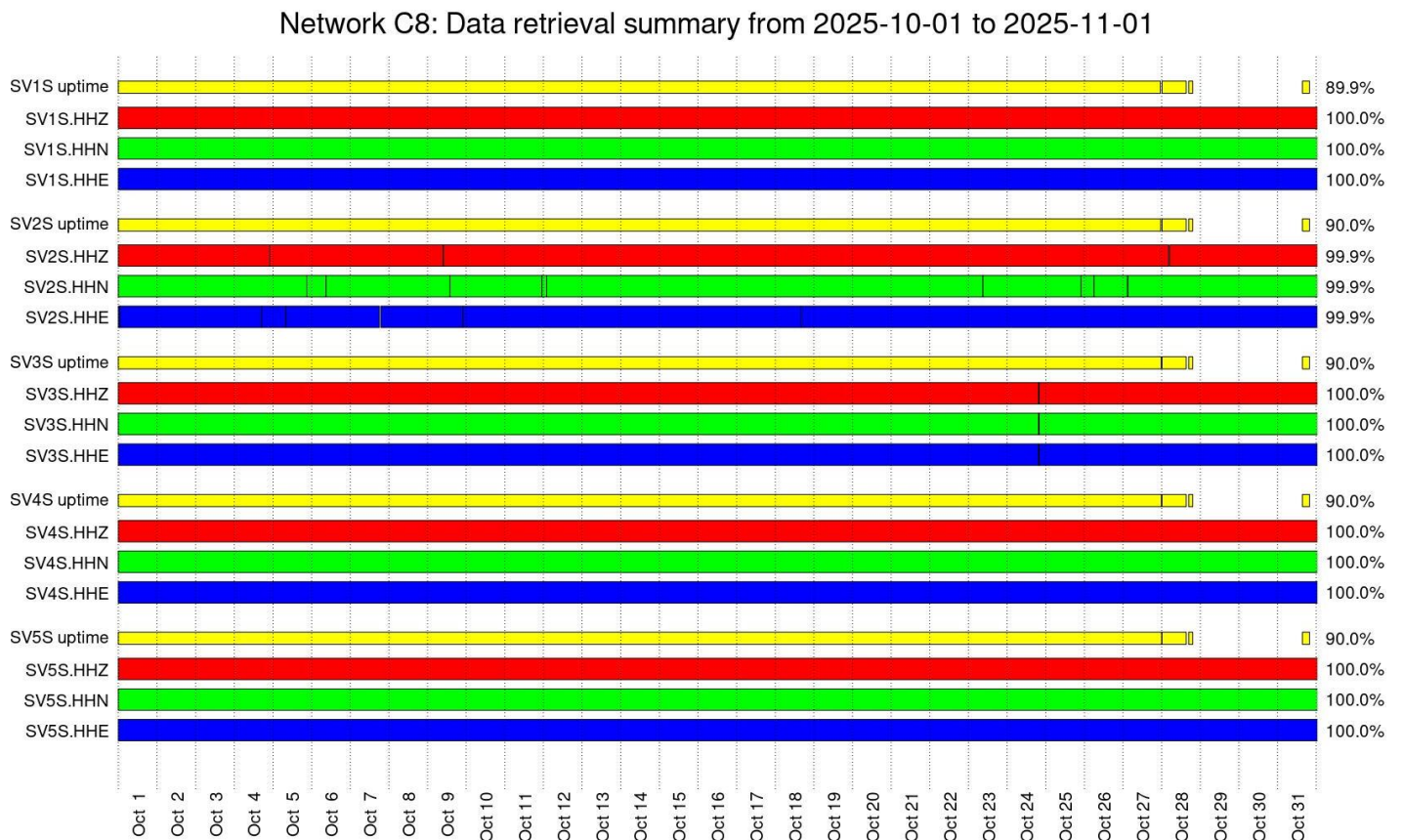


Figure 1. Retrieved data intervals for all channels (red, green, and blue bars) and uptimes (yellow). Total percentages of measured uptime and data retrieval are shown on the right. Gaps in yellow bars show problems with network connections on Oct 29-31 but the data were recovered afterwards.

State of health for station C8.SV1S (NE01) from 2025-10-01 to 2025-11-01
 Power supply voltage

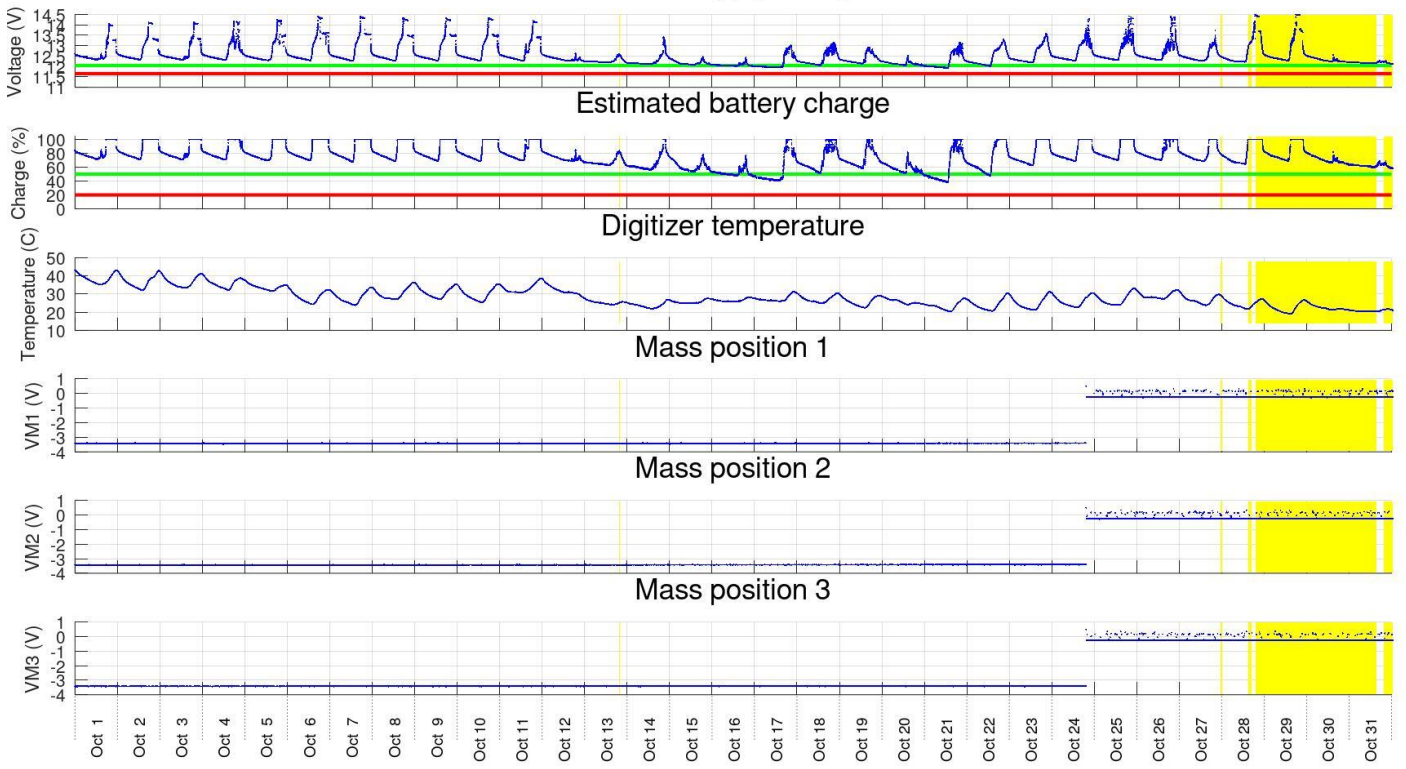
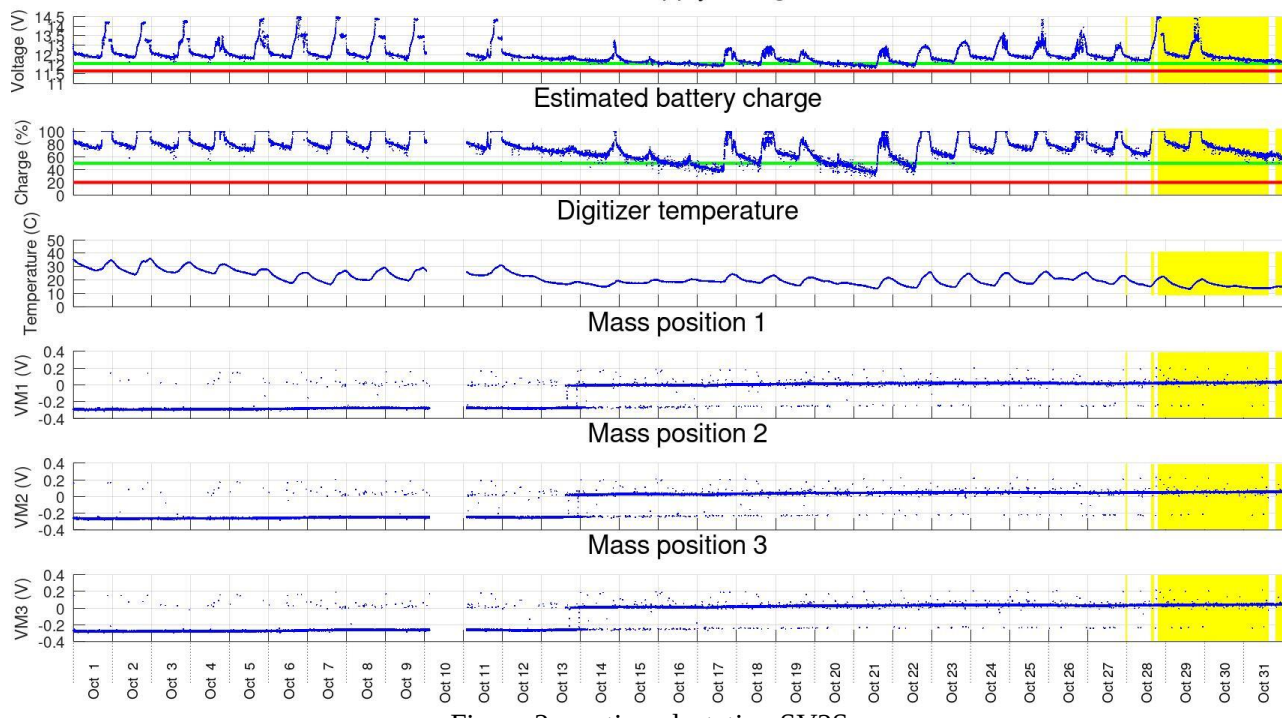


Figure 2. State of health parameters for each station (SV1S here). Image headings: power supply voltage, estimated battery charge levels, temperature on board, voltages measuring mass positions. The gap after October 28 was due to network outage for the whole array.

State of health for station C8.SV2S (SW01) from 2025-10-01 to 2025-11-01

Power supply voltage



State of health for station C8.SV3S (NW01) from 2025-10-01 to 2025-11-01

Power supply voltage

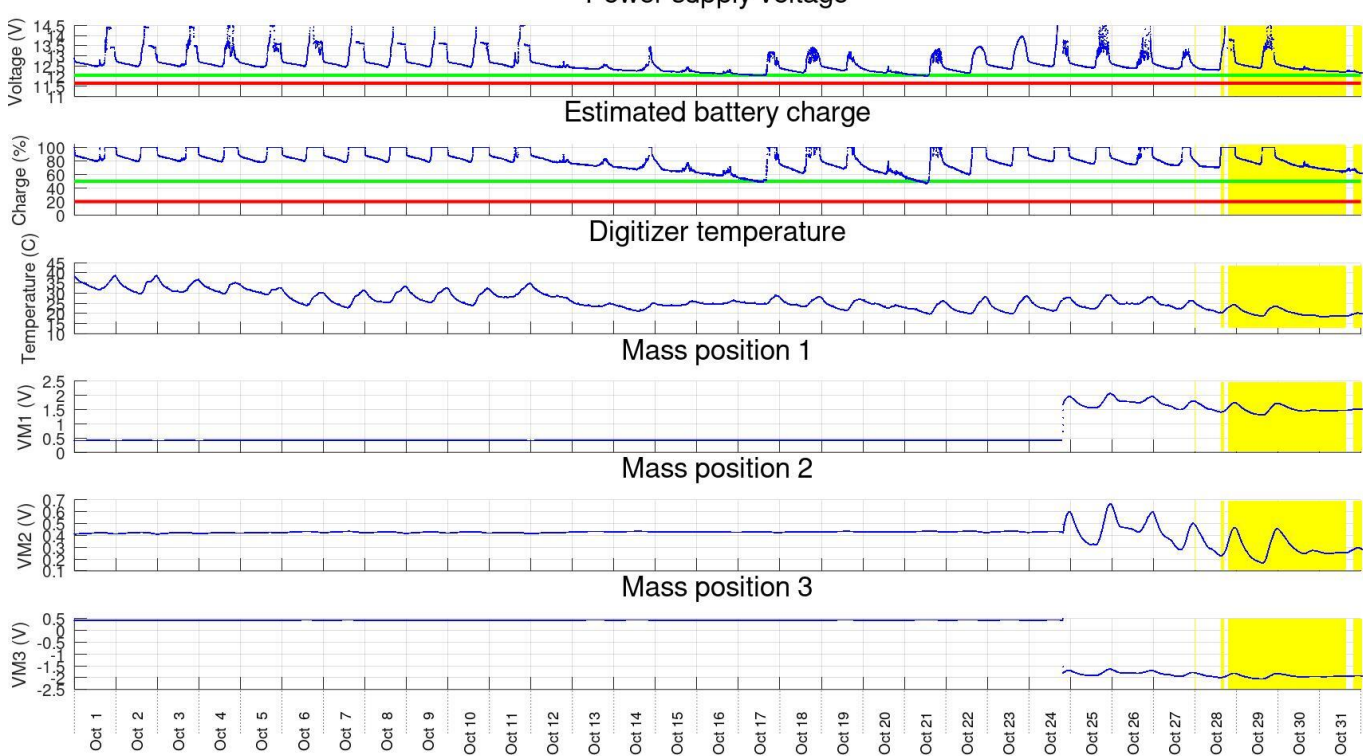


Figure 2, continued, station SV3S.

State of health for station C8.SV4S (SE01) from 2025-10-01 to 2025-11-01
 Power supply voltage

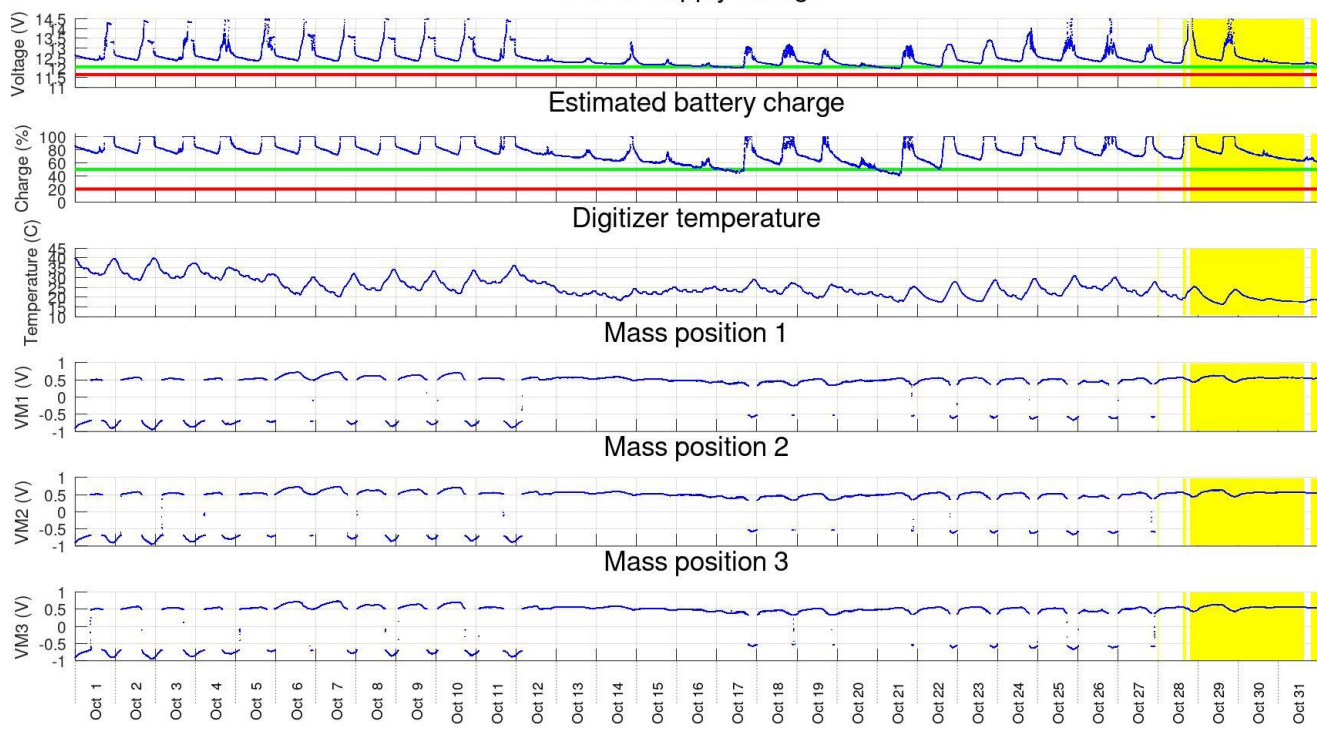


Figure 2, continued, station SV4S.

State of health for station C8.SV5S (NE02) from 2025-10-01 to 2025-11-01

Power supply voltage

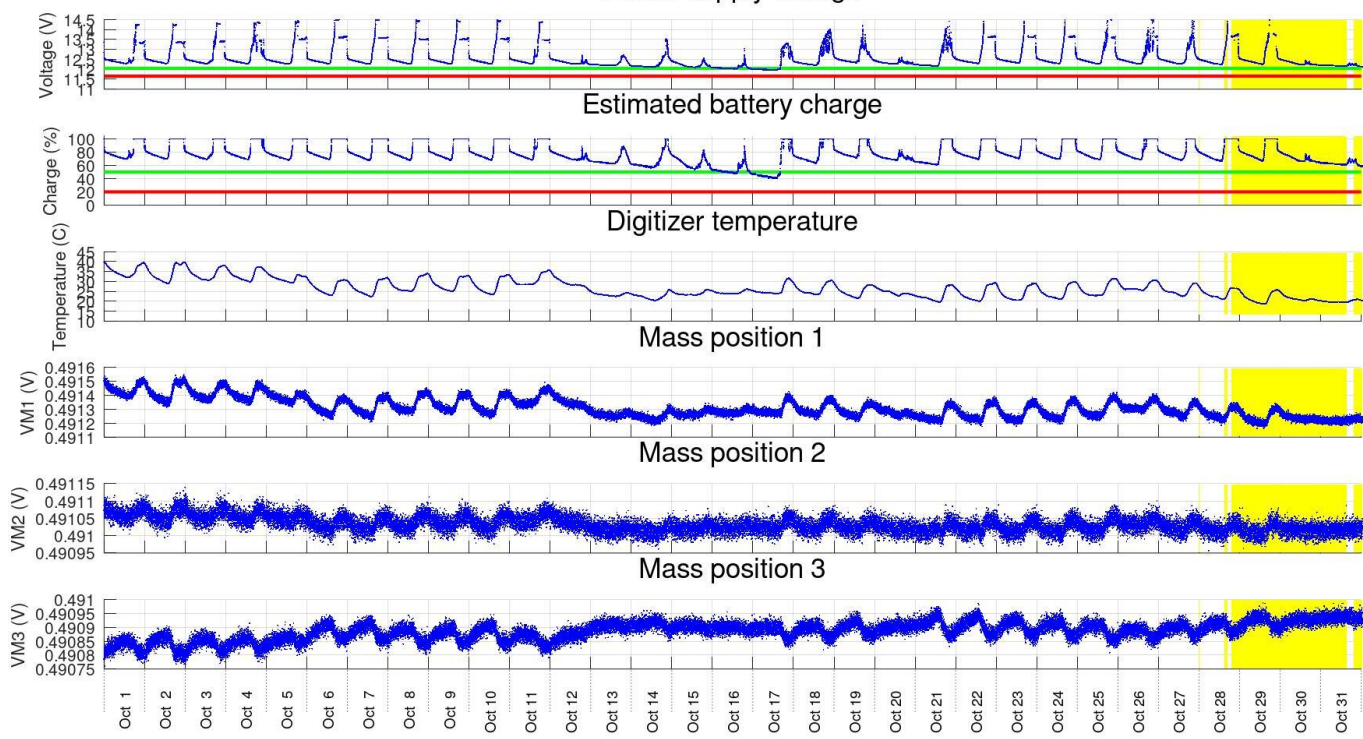


Figure 2, continued, station SV5S.

2. Data quality

Figure 3 shows two measures of data quality evaluated for each channel:

- 1) Numbers of spikes and tears (sharp changes of DC level) within 1-hour time intervals;
- 2) 1-hour root-mean square (RMS) average amplitudes in each channel.

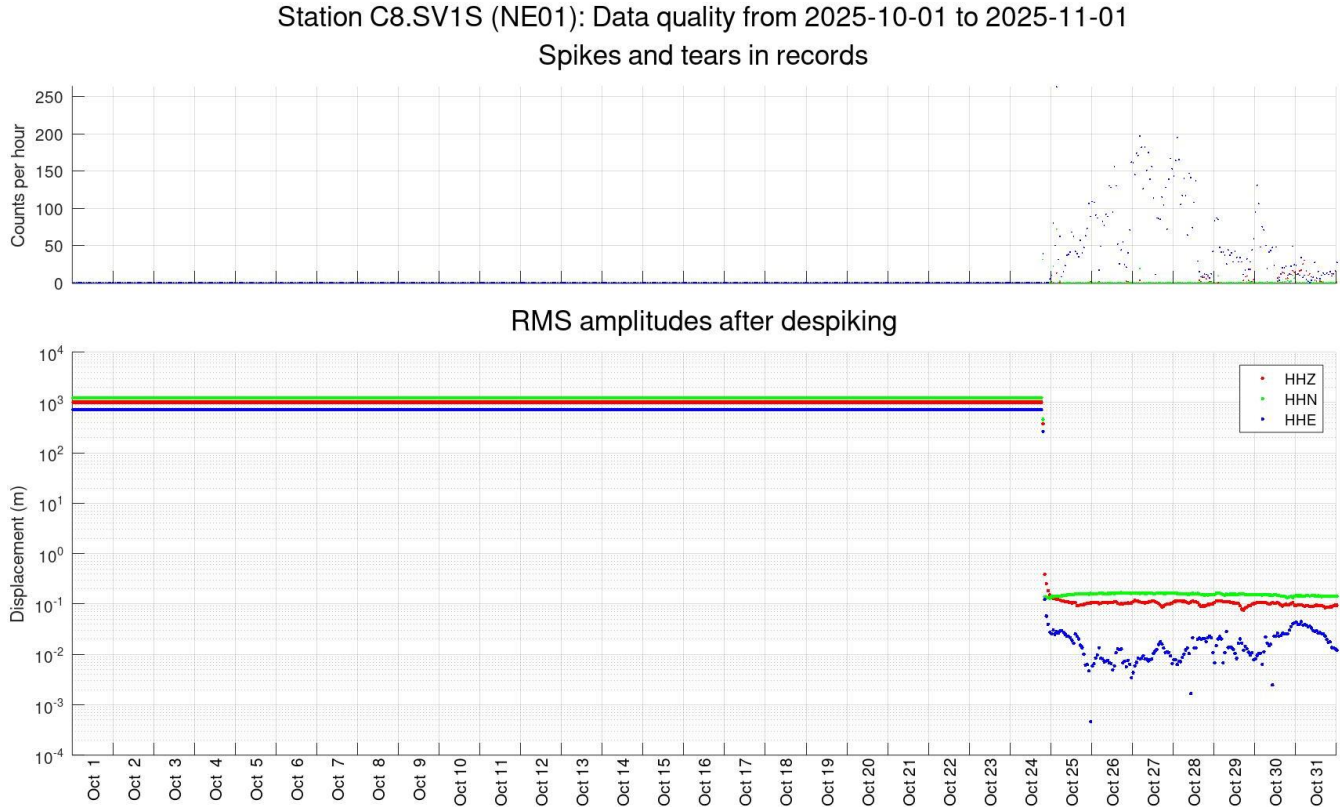


Figure 3. Measures of data quality in hour-long intervals. Station names and time intervals are indicated in plot headings (SV1S in this plot). Red, green, and blue colours correspond to channels HHZ, HHN, and HHE, respectively (as in Figure 1).

Top panels: Numbers of spikes and tears per hour auto-detected in data records.

Bottom panels: RMS ground displacements (meters).

Station C8.SV2S (SW01): Data quality from 2025-10-01 to 2025-11-01
 Spikes and tears in records

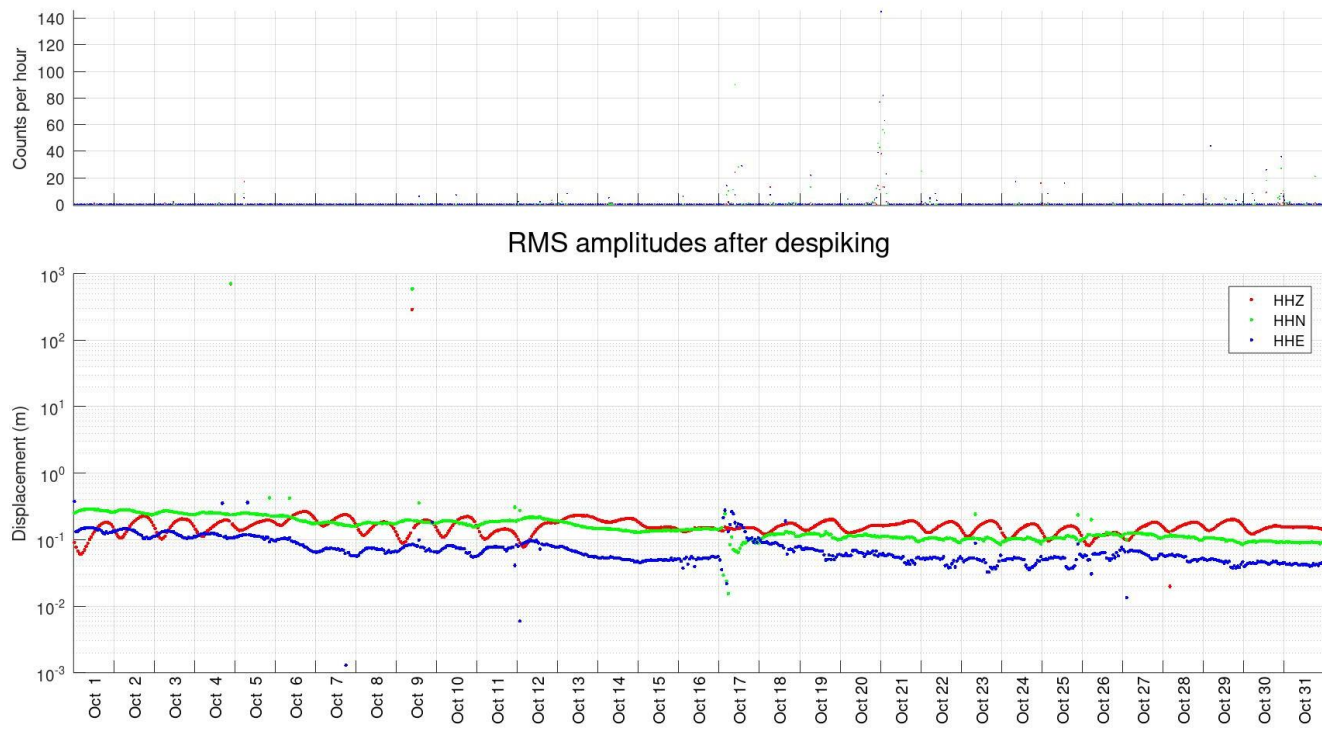


Figure 3, continued. Station SV2S.

Station C8.SV3S (NW01): Data quality from 2025-10-01 to 2025-11-01
 Spikes and tears in records

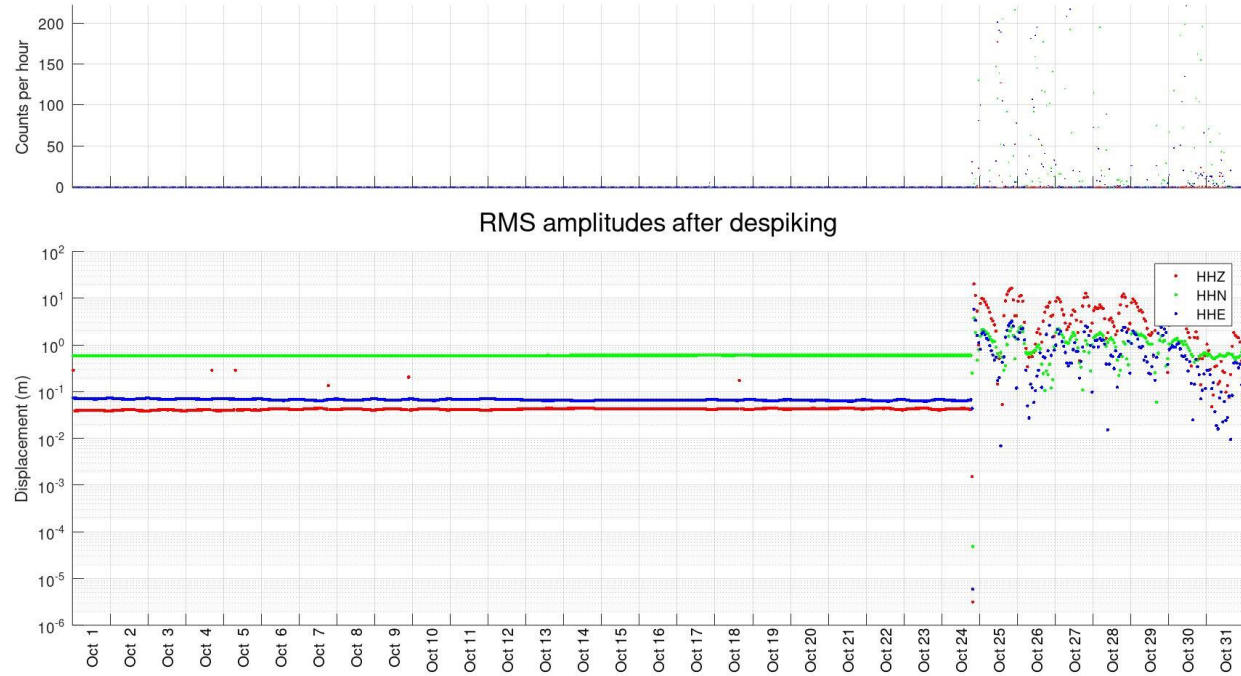


Figure 3, continued. Station SV3S.

Station C8.SV4S (SE01): Data quality from 2025-10-01 to 2025-11-01
 Spikes and tears in records

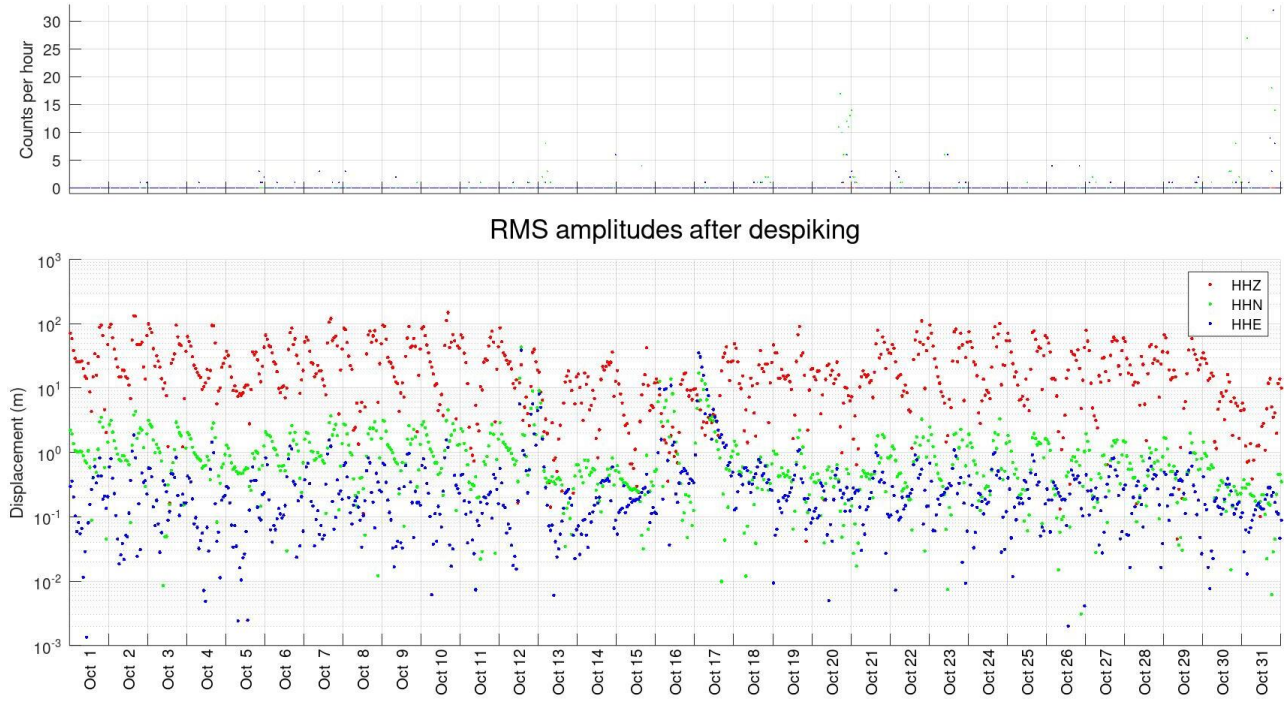


Figure 3, continued. Station SV4S.

Station C8.SV5S (NE02): Data quality from 2025-10-01 to 2025-11-01
 Spikes and tears in records

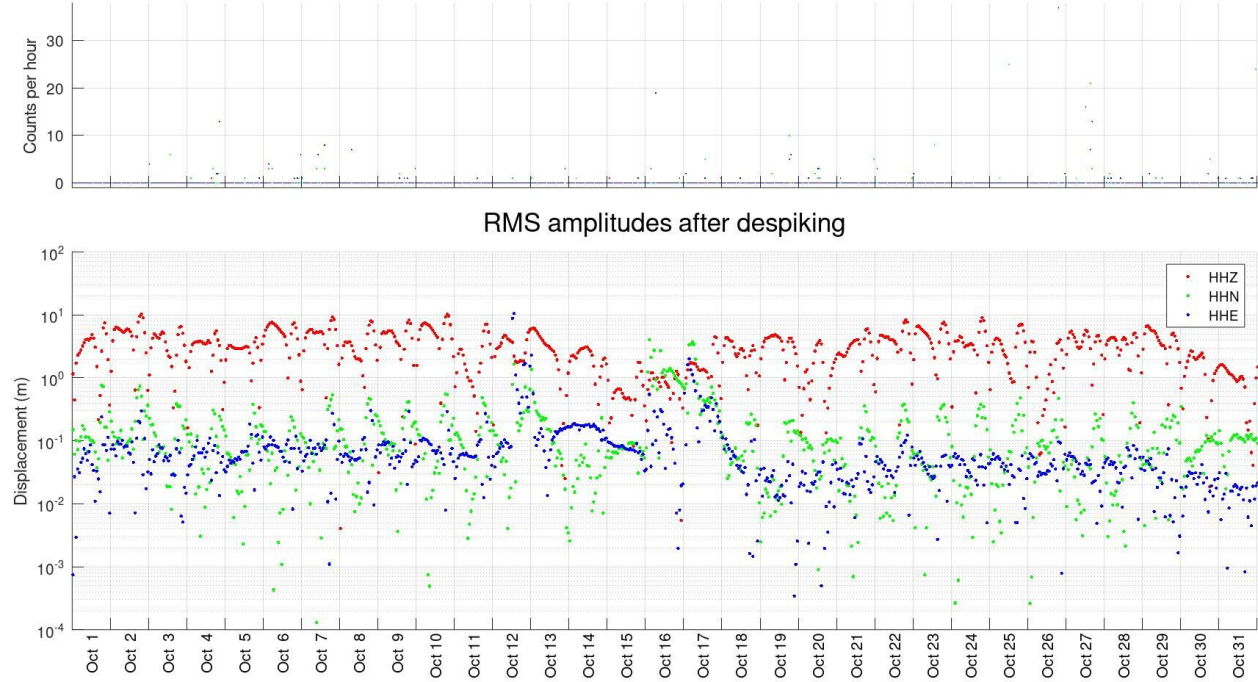


Figure 3, continued. Station SV5S

3. Processing procedure and parameters

The data processing procedure was described in previous reports. Parameters of the STA/LTA algorithm in two frequency bands are shown in Table 1. Only one frequency band (#1) is currently used.

Table 1. STA/LTA algorithm parameters

Parameter	For regional events	For local and target events
Filter band 1	0.5 – 10 Hz	3 – 20 Hz
Filter band 2	3 – 50 Hz	10 – 50 Hz
STA window	3 s	0.2 s
LTA window	15 s	2 s
Floor on normalized STA/LTA ratio	0.5	0.6
Maximum accepted STA/LTA ratio	0.99	0.99
Relative level of triggering	0.5	0.5
Relative level of detriggering	0.5	0.5
Number of channels for triggering	3	3

4. Seismic event detection

The classification of seismic events used in these reports and numbers of events detected in October 2025 are shown in Table 2.

Table 2. Classification of seismic events detected at Aquistore broadband seismic array

Event class code	Class name	Identification criteria	Number of detections in this report
1	Teleseismic	Hypocentral distance $D > 1000$ km, presence in catalogues	30
2	Regional	$100 < D < 1000$ km, presence in catalogues	1
3	Local	Approx. $4 < D < 100$ km	-----
3a	Possible mine blasts	Characteristic waveforms, amplitudes, back-azimuths east of Aquistore,	10

		<i>D</i> about 12-15 km	
3b	Mining-related	Low frequencies, extended repeated wavetrains low arrival velocities related to surface waves	6 (selected from numerous occurrences)
4	Proximity (close local)	$D < 3-4$ km, deviation of array moveouts from plane-wave patterns, high frequency	-----
4a*	Surface sources near array	Large travel-time moveouts, variable back-azimuths	1*
4b*	Target zone	Source at recognizable nonzero depth, small travel-time moveouts, high frequency	0*

*) Because of using only three stations, classes 4a and 4b are not differentiated in current report.

Automatic detections

The procedure of multichannel automatic detections is currently being revised and not shown in the present report.

Event bulletins

Earthquake data bulletins for the period of this report were obtained from NEIC (USGS) and NRCAN web services (Figure 5). Events larger than magnitude 2.5 were taken from USGS, and all available events obtained from NRCAN. Events with magnitudes above the selected $magnitude \propto distance^{1.5}$ threshold (dashed green line in Figure 5) were reviewed interactively (next section).

Events from 2025-10-01 to 2025-11-01
 20 regional
 1591 teleseismic

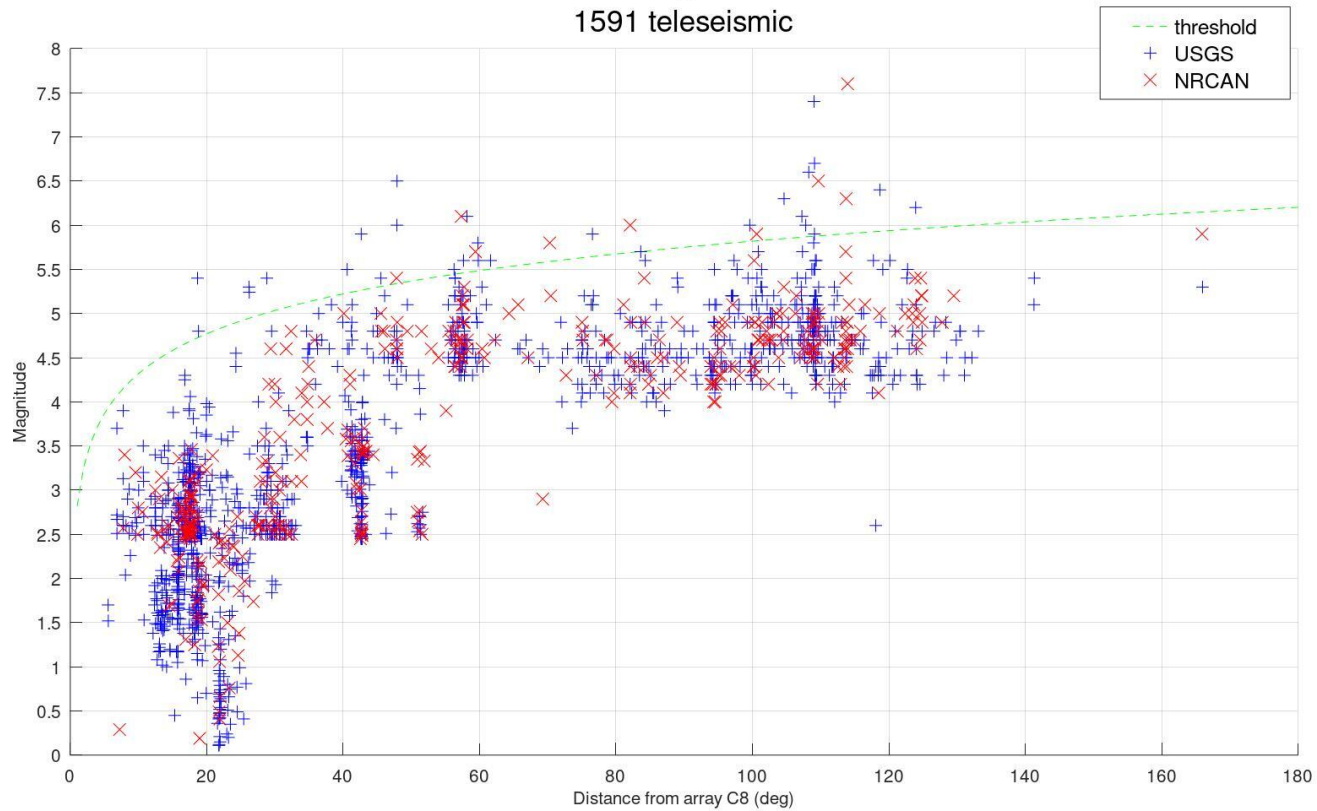


Figure 5. Magnitudes and distances from Aquistore for earthquake parameters downloaded from USGS and NRCAN databases (legend). Dashed green line shows the detection threshold above which a manual review of events was performed.

Teleseismic events (class 1)

Above the threshold line in Figure 5, 30 teleseismic events (class 1 in Table 2) were identified in October 2025 (Figure 6).

Time zeros in Figure 6 plots are located at the times of P-wave arrivals at the Aquistore array predicted in the reference model IASP91, and blue bars near *time* = 0 are interactive picks of P-wave arrival times.

Note that the records from station SV3S are extremely noisy (and actually, low-amplitude) at the beginning of the month. After replacing the sensor cable on about October 20, SV3S records look normal.

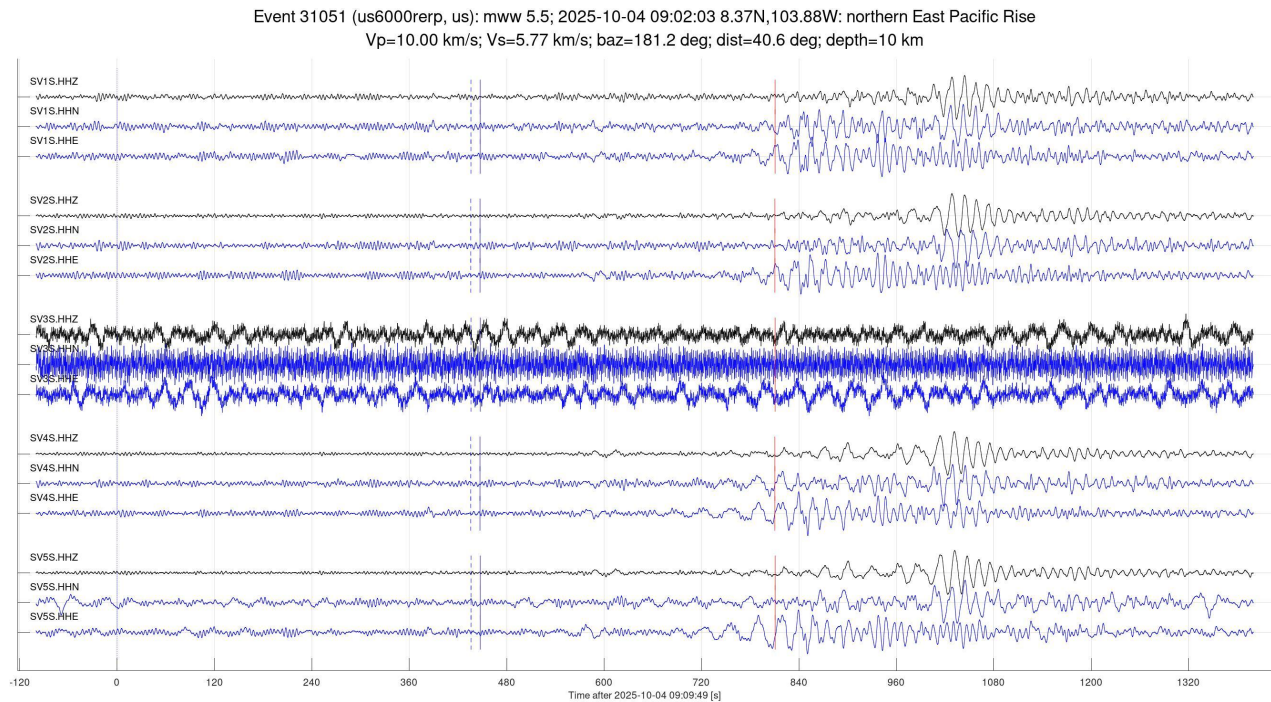


Figure 6. Sample teleseismic events detected at Aquistore in October 2025. Catalogue IDs, times, distances in degrees, source coordinates and localities, back-azimuths ('baz='), distances ('dist=') and source depths are shown in plot headings. Vertical-component records are shown in black, and horizontal components in blue.

Event 31073 (us6000rei1, us): mww 6.1; 2025-10-03 16:07:45 51.64N,160.02E: 181 km SE of Vilyuchinsk, Russia
 Vp=10.00 km/s; Vs=5.77 km/s; baz=312.7 deg; dist=57.3 deg; depth=19 km

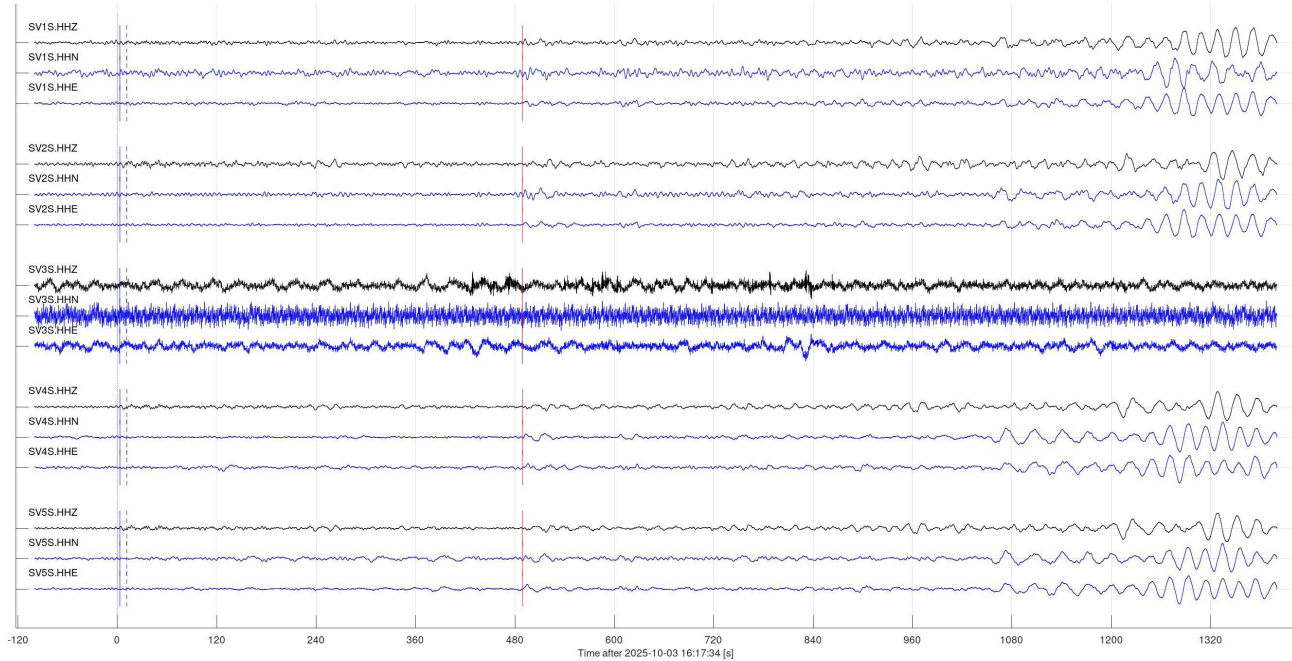


Figure 6, continued.

Event 31135 (us6000resn, us): mww 5.9; 2025-10-04 15:21:09 37.43N,141.64E: 56 km E of Tomioka, Japan
 Vp=10.00 km/s; Vs=5.77 km/s; baz=312.3 deg; dist=76.5 deg; depth=44 km

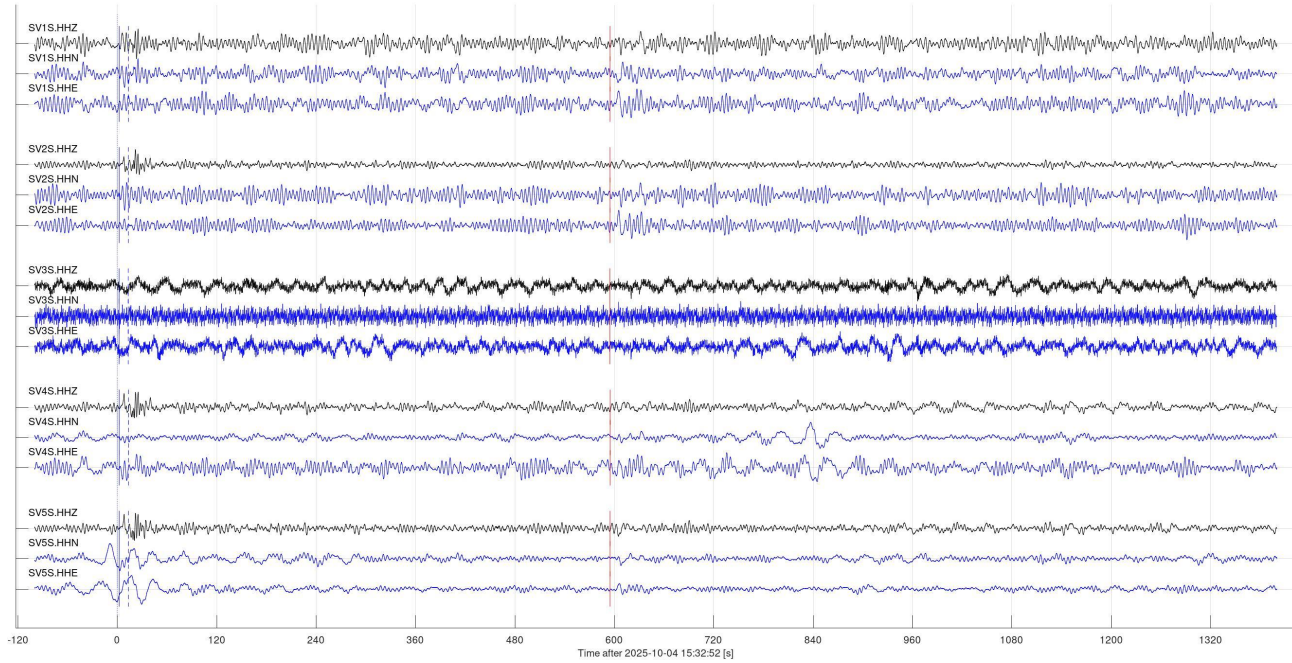


Figure 6, continued.

Event 31318 (us6000rb2, us): mww 6.6; 2025-10-07 11:05:18 6.78S,146.77E: 26 km WSW of Lae, Papua New Guinea
 $V_p=10.00$ km/s; $V_s=5.77$ km/s; $\text{baz}=281.0$ deg; $\text{dist}=108.3$ deg; $\text{depth}=99$ km

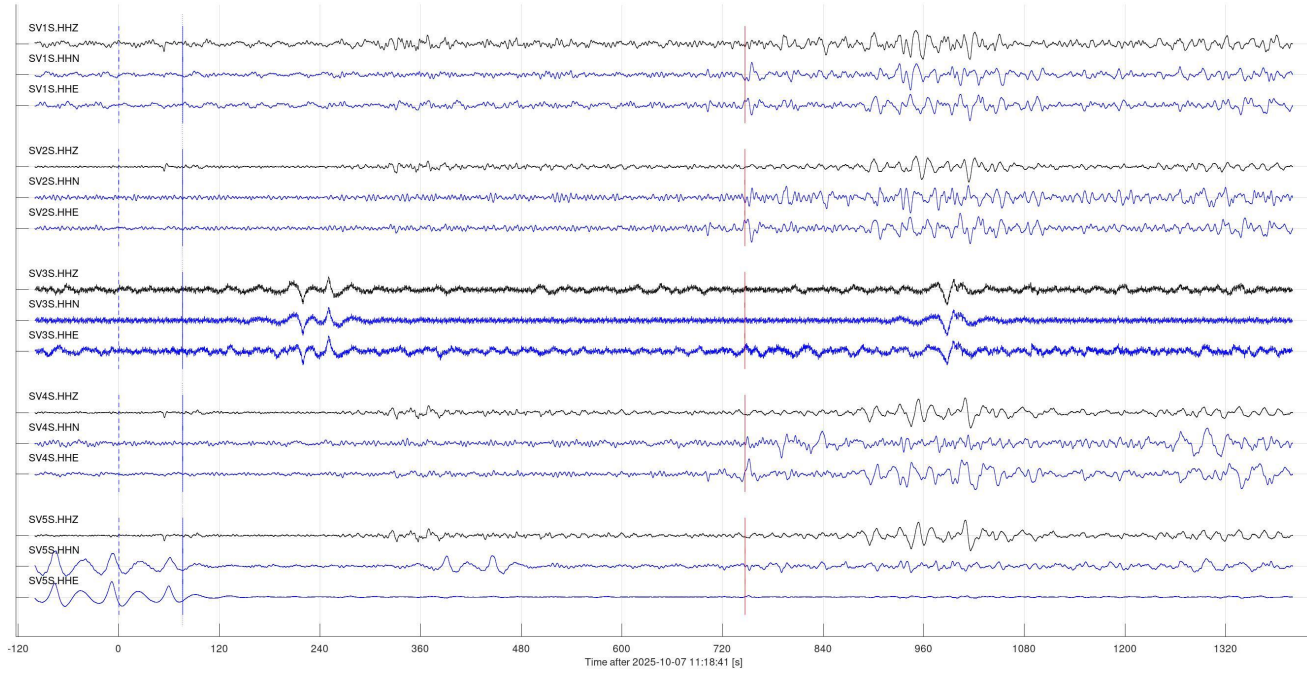


Figure 6, continued.

Event 31401 (us6000rfye, us): mww 6.3; 2025-10-10 02:08:11 3.03S,147.97E: 134 km SE of Lorengau, Papua New Guinea
 $V_p=10.00$ km/s; $V_s=5.77$ km/s; $\text{baz}=282.5$ deg; $\text{dist}=104.6$ deg; $\text{depth}=10$ km

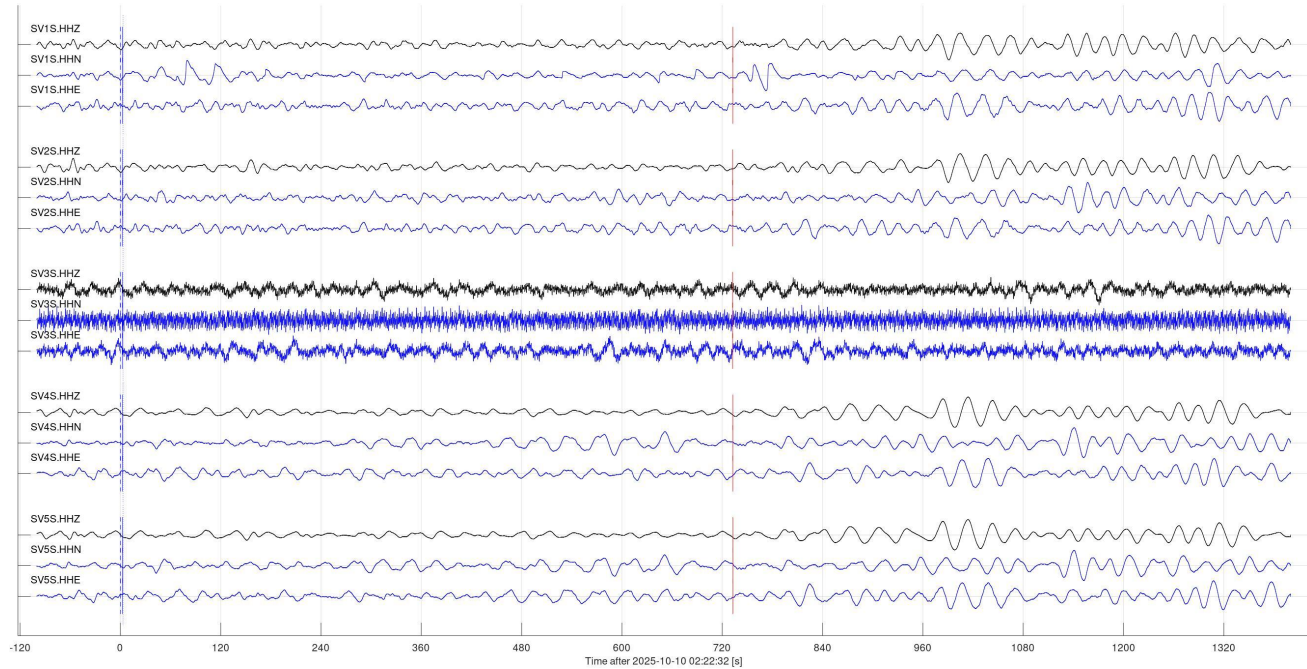


Figure 6, continued.

Event 31402 (us6000rfx2, us): mb 5.9; 2025-10-10 01:51:15 7.10N,126.89E: 40 km ESE of Manay, Philippines
 $V_p=10.00$ km/s; $V_s=5.77$ km/s; $\text{baz}=306.5$ deg; $\text{dist}=109.1$ deg; depth=62 km

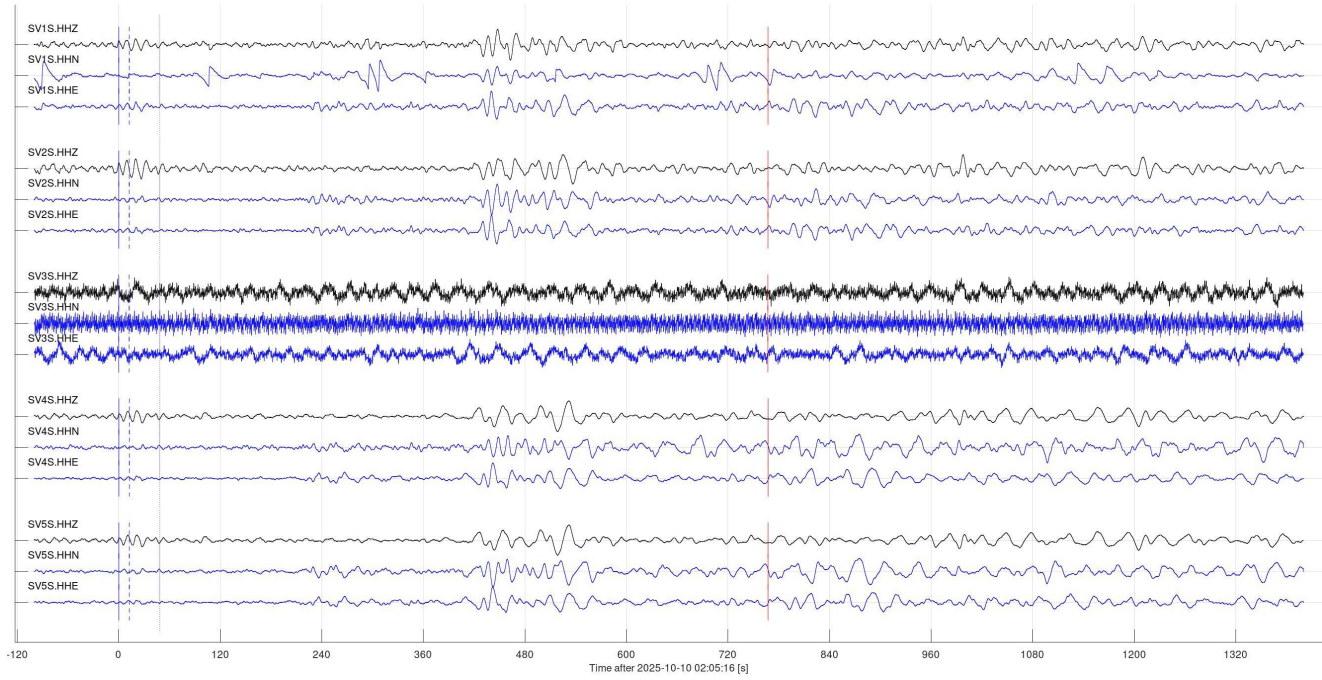


Figure 6, continued.

Event 31403 (us6000rfwz, us): mww 7.4; 2025-10-10 01:44:00 7.26N,126.75E: 20 km E of Santiago, Philippines
 $V_p=10.00$ km/s; $V_s=5.77$ km/s; $\text{baz}=306.7$ deg; $\text{dist}=109.0$ deg; depth=58 km

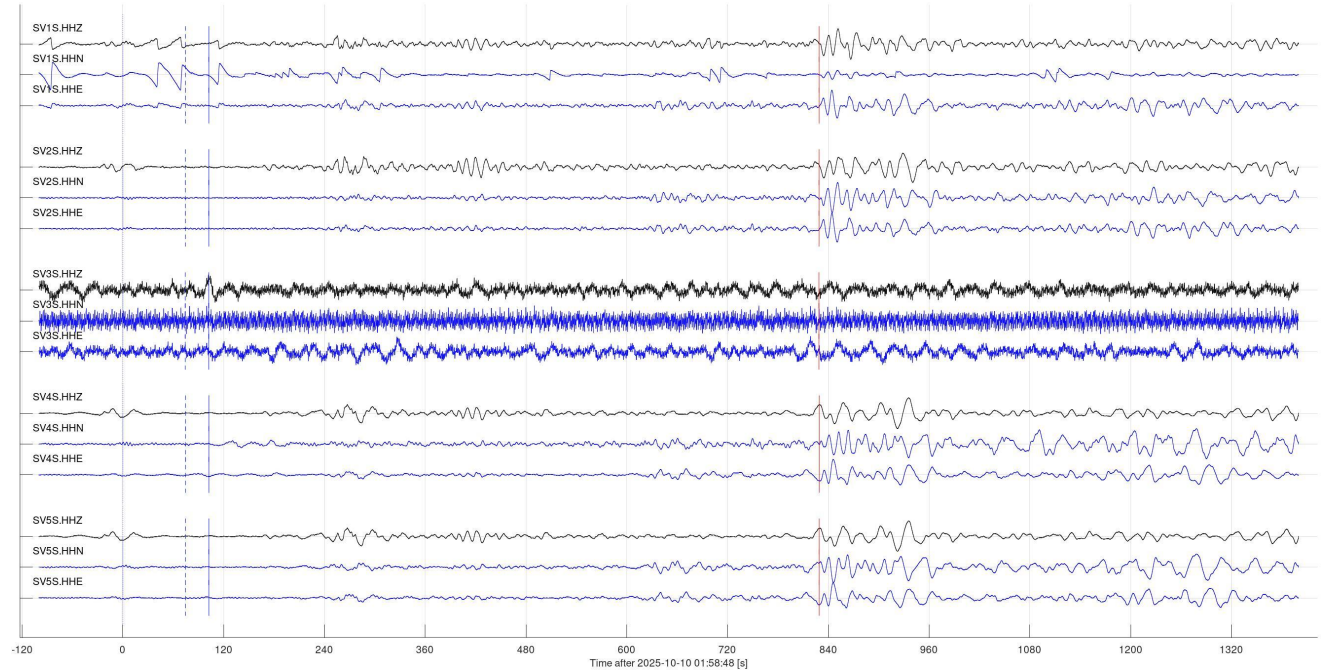


Figure 6, continued.

Event 31461 (us6000rgf4, us): mww 7.6; 2025-10-10 20:29:21 60.20S,61.80W: Drake Passage
 $V_p=10.00$ km/s; $V_s=5.77$ km/s; $\text{baz}=158.9$ deg; $\text{dist}=114.0$ deg; $\text{depth}=8.79$ km

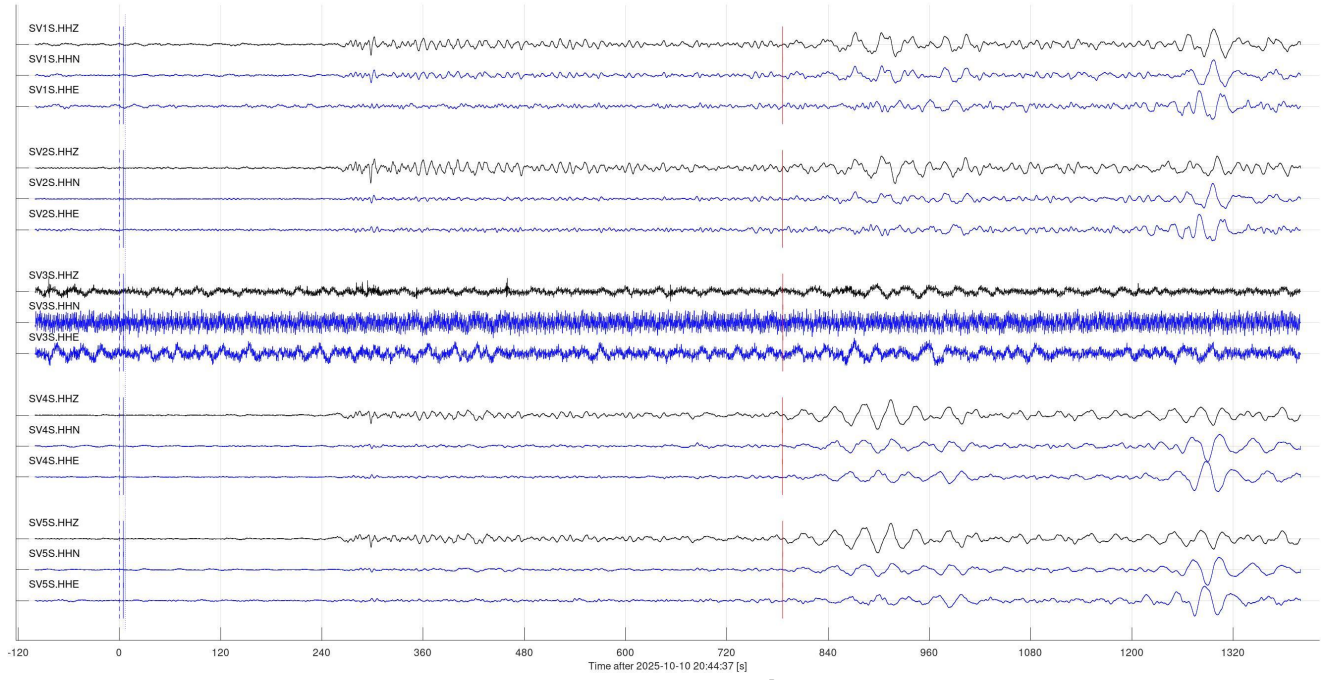


Figure 6, continued.

Event 31483 (us6000rg2s, us): mb 5.6; 2025-10-10 11:16:02 50.38N,156.52E: 43 km SE of Severo-Kuril'sk, Russia
 $V_p=10.00$ km/s; $V_s=5.77$ km/s; $\text{baz}=313.2$ deg; $\text{dist}=59.8$ deg; $\text{depth}=76$ km

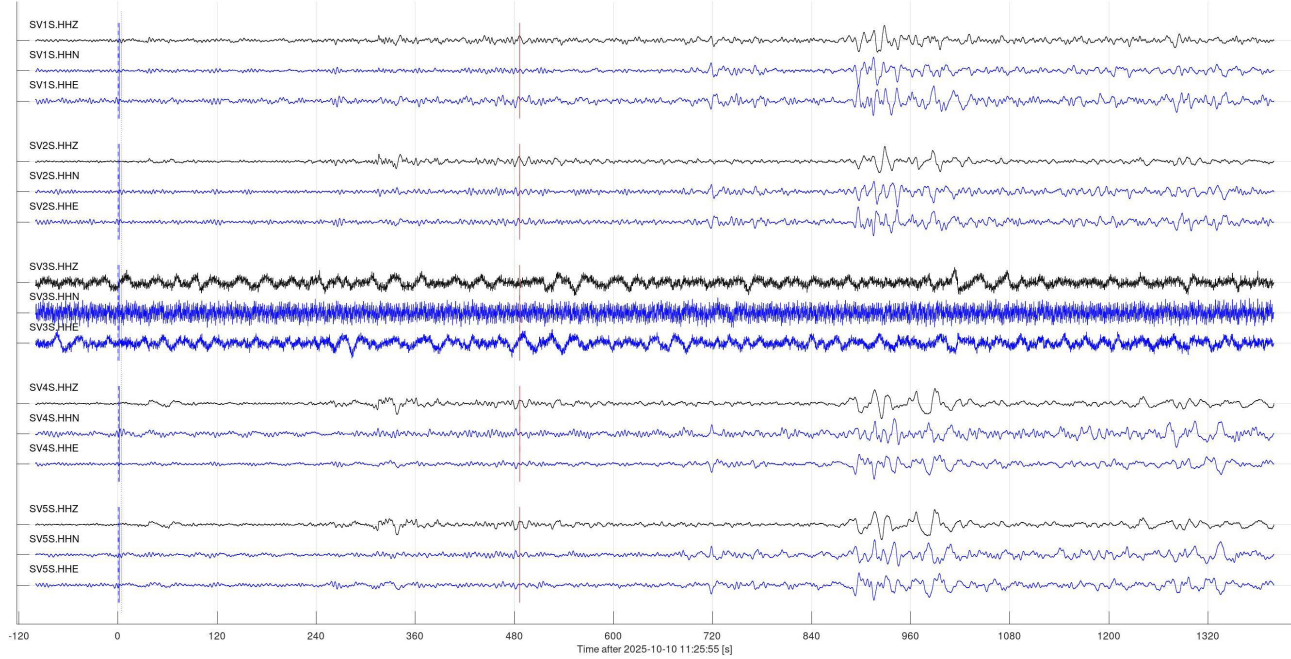


Figure 6, continued.

Event 31484 (us6000rg2r, us): mww 6.7; 2025-10-10 11:12:07 7.17N,126.76E: 23 km ESE of Santiago, Philippines
 Vp=10.00 km/s; Vs=5.77 km/s; baz=306.6 deg; dist=109.1 deg; depth=61 km

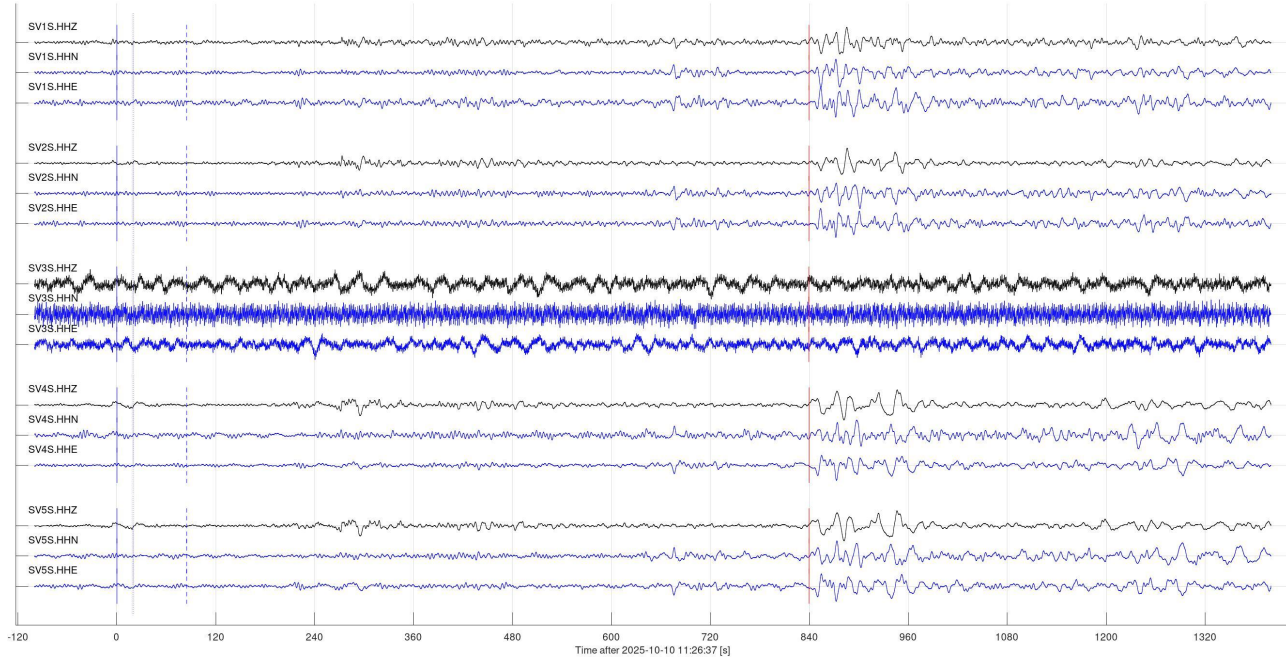


Figure 6, continued.

Event 31538 (us6000rgkkr, us): mww 6.0; 2025-10-11 14:32:59 8.92N,126.40E: 10 km ENE of Aras-asan, Philippines
 Vp=10.00 km/s; Vs=5.77 km/s; baz=307.9 deg; dist=107.8 deg; depth=59 km

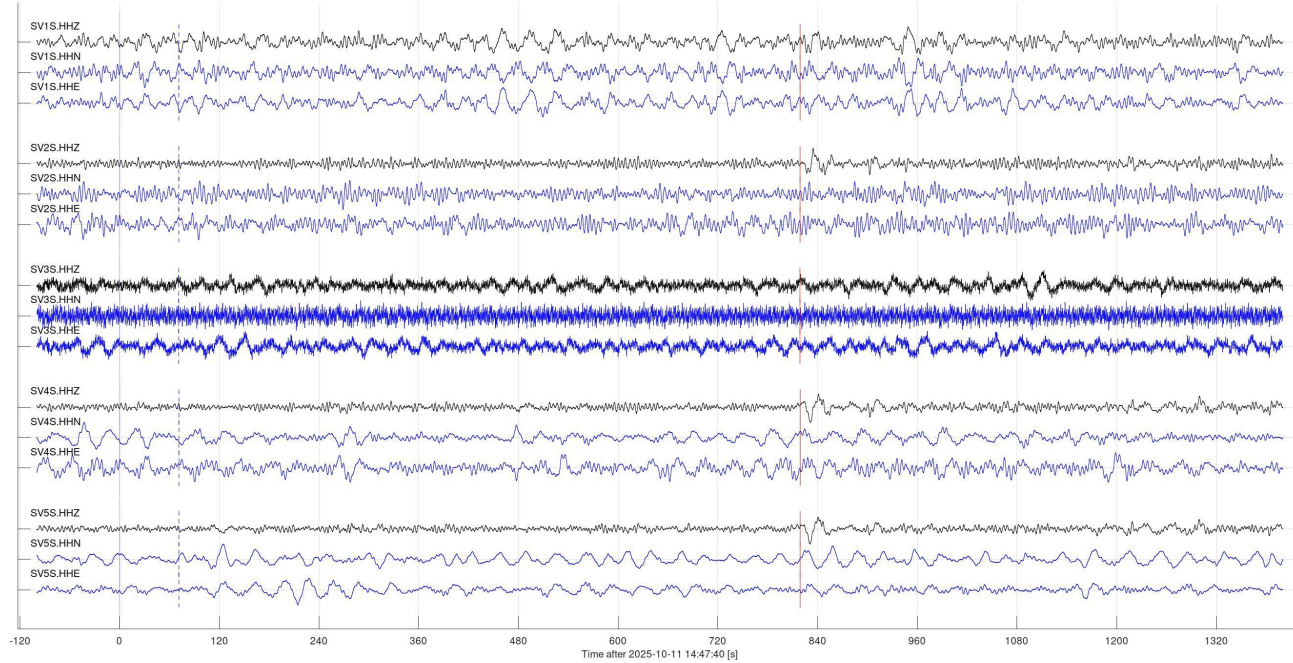


Figure 6, continued.

Event 31699 (us6000rhg5, us): mww 6.5; 2025-10-16 05:48:55 2.17S,138.94E: 194 km WNW of Abepura, Indonesia
 Vp=10.00 km/s; Vs=5.77 km/s; baz=290.4 deg; dist=109.7 deg; depth=35 km

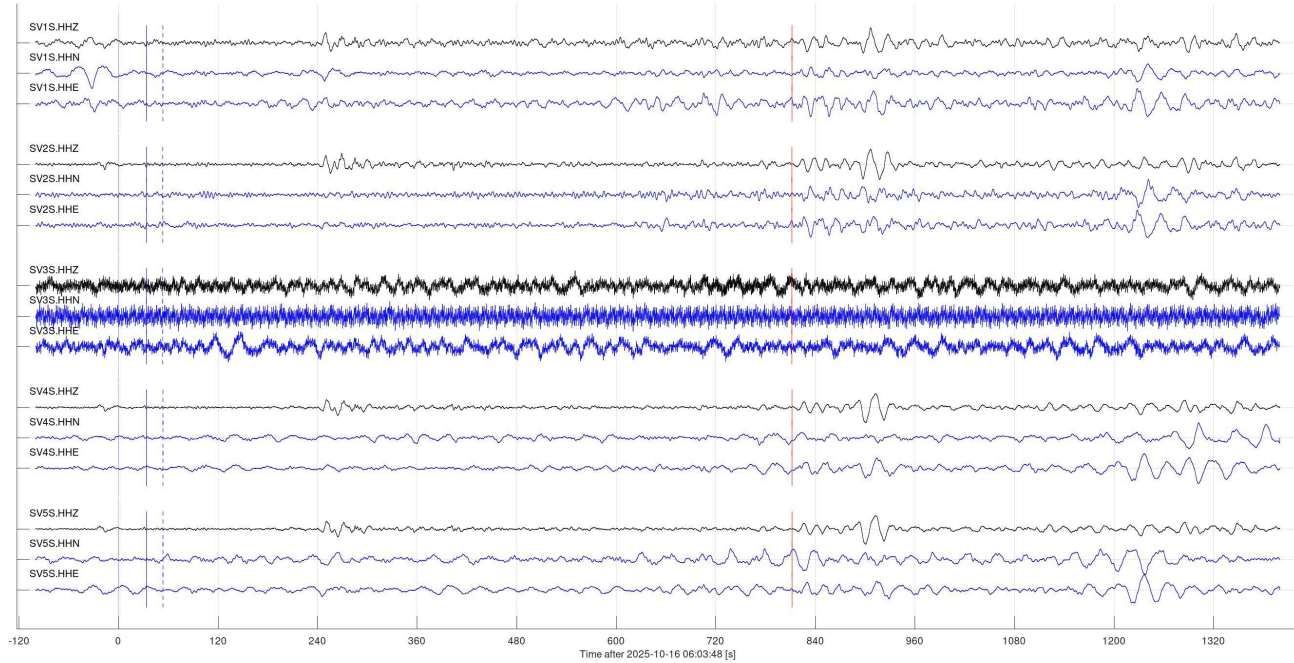


Figure 6, continued.

Event 31708 (us6000rhf2, us): mww 6.3; 2025-10-16 01:42:33 59.91S,61.62W: Drake Passage
 Vp=10.00 km/s; Vs=5.77 km/s; baz=158.6 deg; dist=113.7 deg; depth=10 km

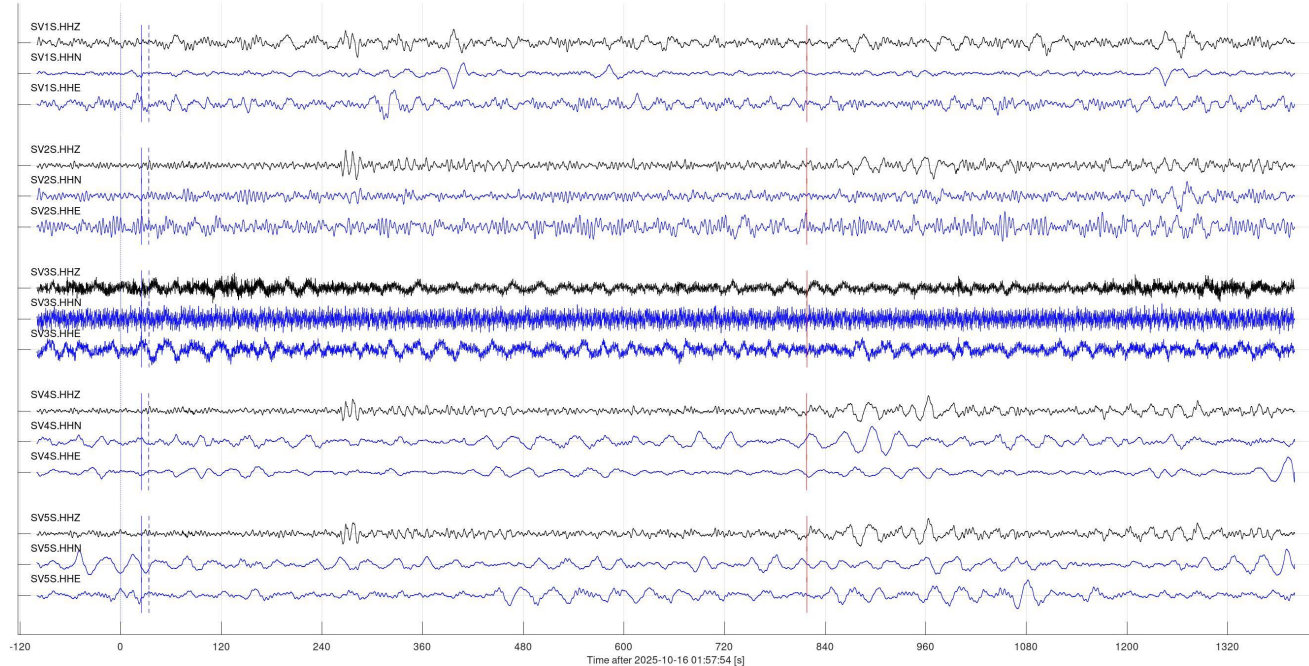


Figure 6, continued.

Event 31768 (us6000rhns, us): mww 6.1; 2025-10-16 23:03:16 9.76N,126.11E: 0 km WSW of Union, Philippines
 Vp=10.00 km/s; Vs=5.77 km/s; baz=308.6 deg; dist=107.3 deg; depth=69 km

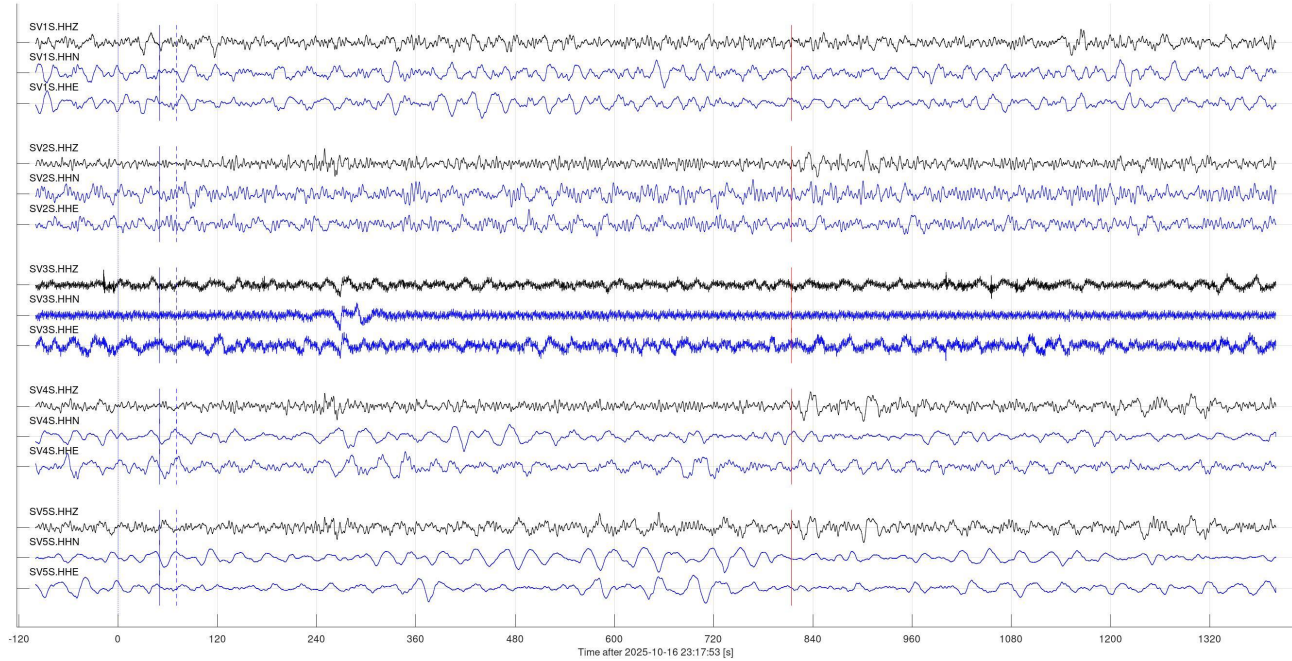


Figure 6, continued.

Event 31985 (us6000risn, us): mww 5.6; 2025-10-23 02:31:28 51.39N,159.65E: 191 km SSE of Vilyuchinsk, Russia
 Vp=10.00 km/s; Vs=5.77 km/s; baz=312.6 deg; dist=57.6 deg; depth=10 km

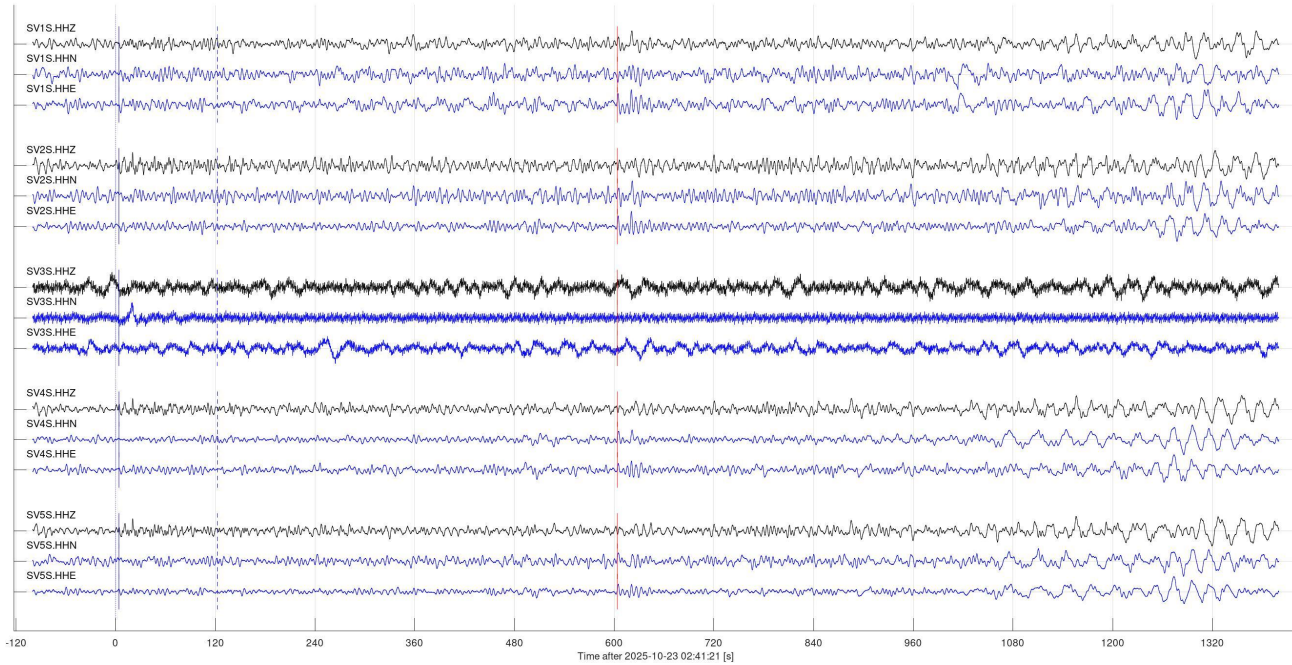


Figure 6, continued.

Event 32011 (us6000ril5, us): mww 5.9; 2025-10-22 03:57:08 9.37N,84.18W: 7 km SSW of Quepos, Costa Rica
 Vp=10.00 km/s; Vs=5.77 km/s; baz=151.9 deg; dist=42.6 deg; depth=31 km

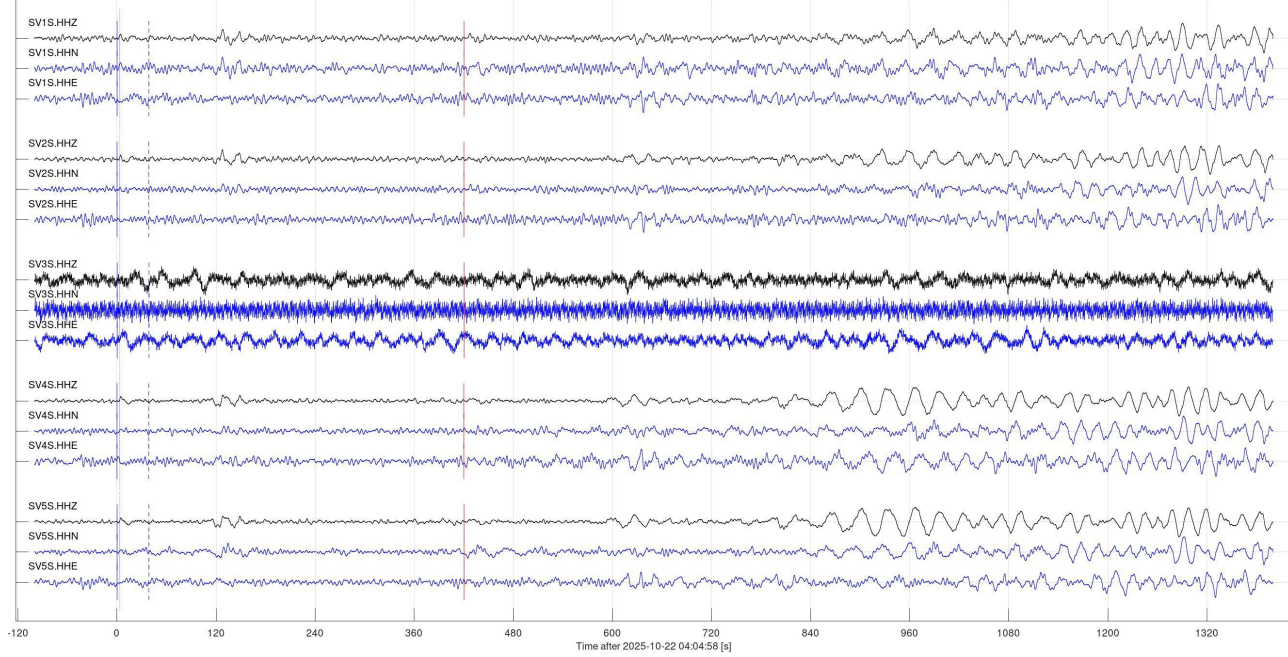


Figure 6, continued.

Event 32017 (us6000rik7, us): mww 5.5; 2025-10-22 00:05:44 3.62S,79.81W: 16 km WNW of Piñas, Ecuador
 Vp=10.00 km/s; Vs=5.77 km/s; baz=151.7 deg; dist=56.3 deg; depth=74 km

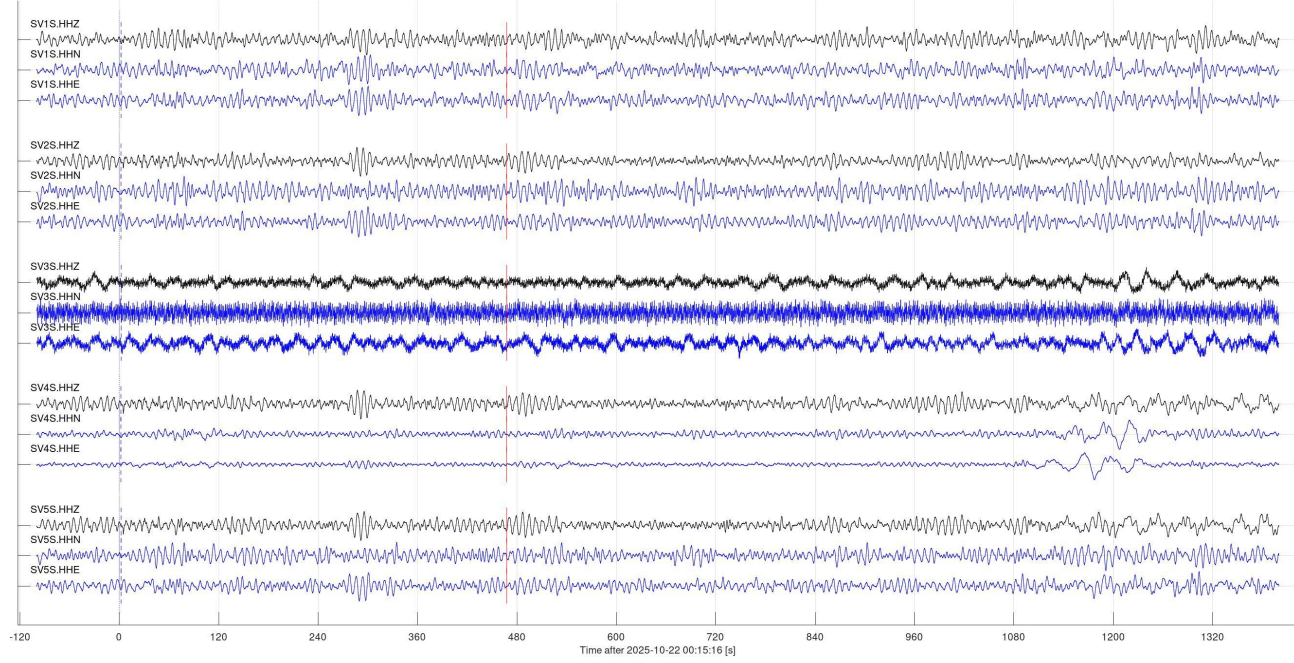


Figure 6, continued.

Event 32141 (us6000rje7, us): mww 5.3; 2025-10-25 06:34:01 71.64N,131.88W: Beaufort Sea
 $V_p=10.00$ km/s; $V_s=5.77$ km/s; $\text{baz}=339.8$ deg; $\text{dist}=26.2$ deg; $\text{depth}=7.75$ km

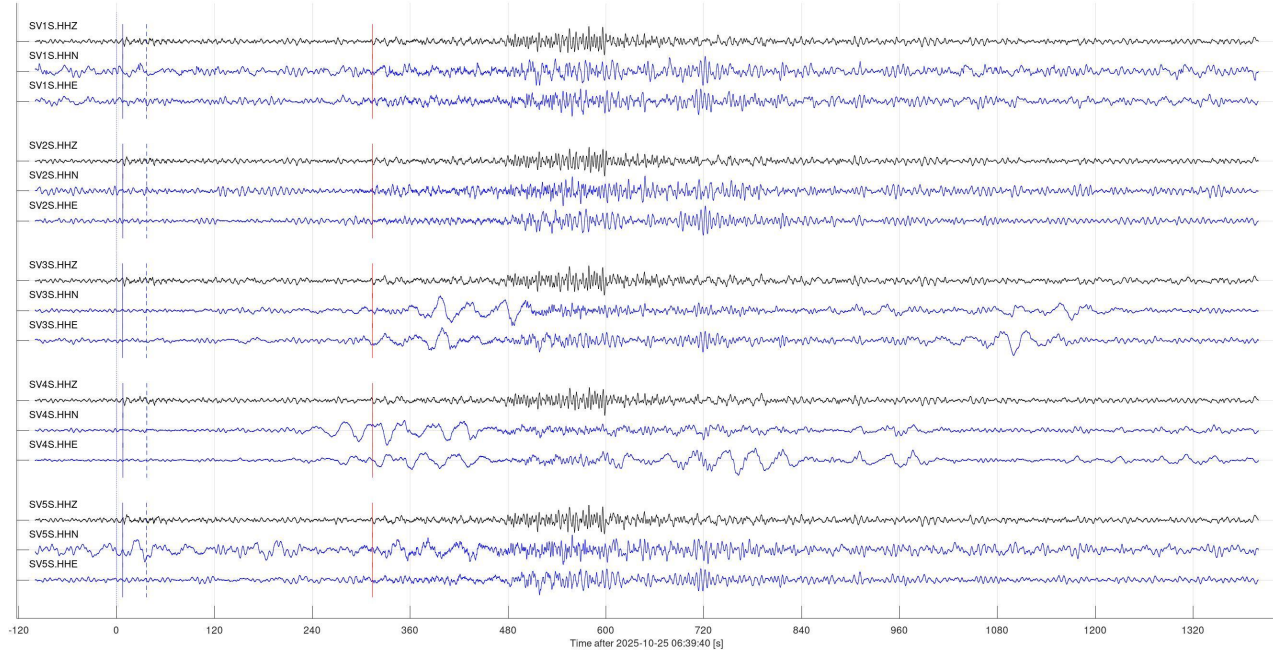


Figure 6, continued.

Event 32159 (us6000rj9f, us): mww 5.8; 2025-10-24 16:40:10 43.00N,145.64E: 35 km S of Nemuro, Japan
 $V_p=10.00$ km/s; $V_s=5.77$ km/s; $\text{baz}=313.4$ deg; $\text{dist}=70.3$ deg; $\text{depth}=41$ km

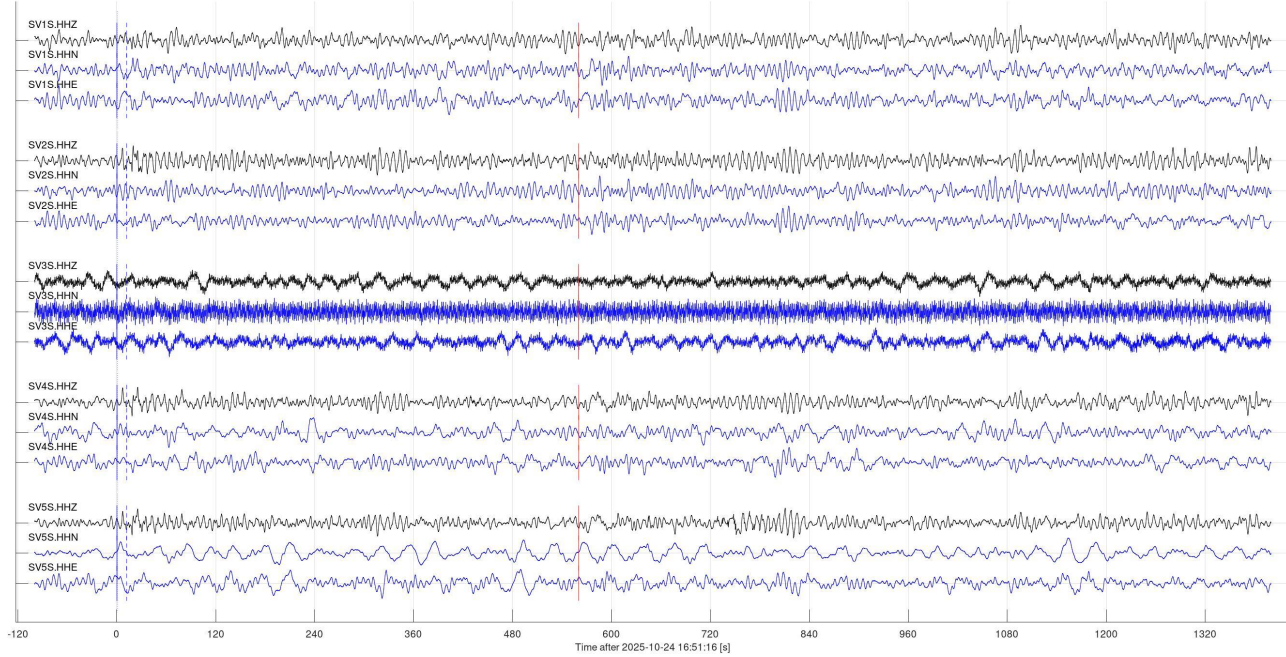


Figure 6, continued.

Event 32174 (20251025.0634006, cn): -- 5.2; 2025-10-25 06:34:03 71.66N,132.01W: 248 km N of Tuktoyaktuk NT
 $V_p=10.00$ km/s; $V_s=5.77$ km/s; $\text{baz}=339.7$ deg; $\text{dist}=26.2$ deg; $\text{depth}=30$ km

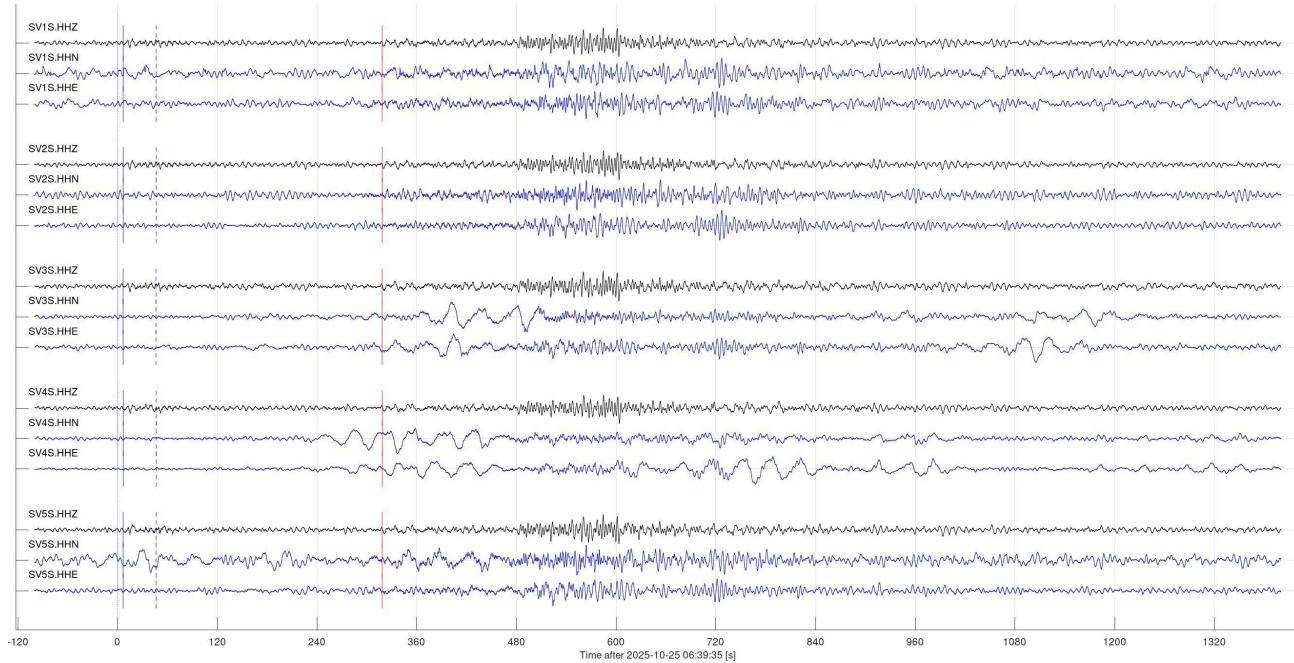


Figure 6, continued.

Event 32207 (us6000rjhm, us): mww 6.0; 2025-10-25 23:28:05 12.41S, 166.39E: 197 km SSE of Lata, Solomon Islands
 $V_p=10.00$ km/s; $V_s=5.77$ km/s; $\text{baz}=262.2$ deg; $\text{dist}=99.6$ deg; $\text{depth}=54$ km

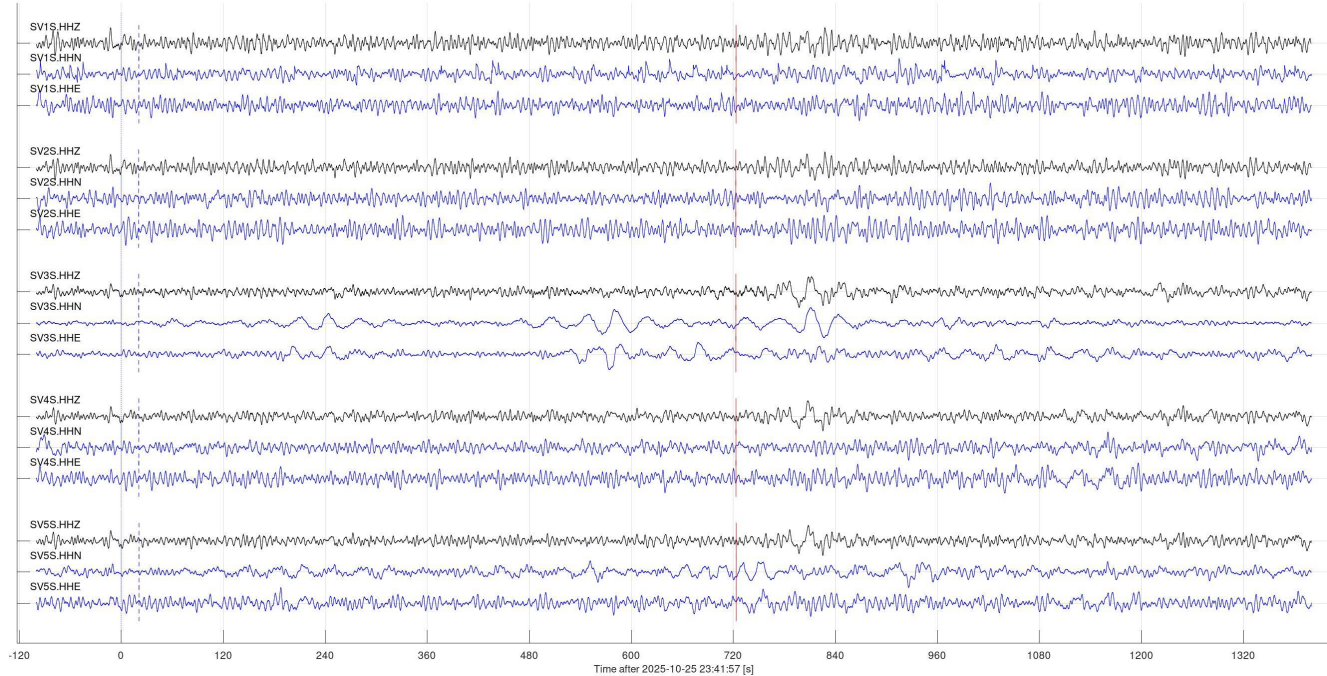


Figure 6, continued.

Event 32277 (us6000rjvf, us): mww 5.7; 2025-10-28 07:06:26 50.38N,157.39E: 95 km ESE of Severo-Kuril'sk, Russia
 $V_p=10.00$ km/s; $V_s=5.77$ km/s; $\text{baz}=312.8$ deg; $\text{dist}=59.4$ deg; $\text{depth}=46$ km

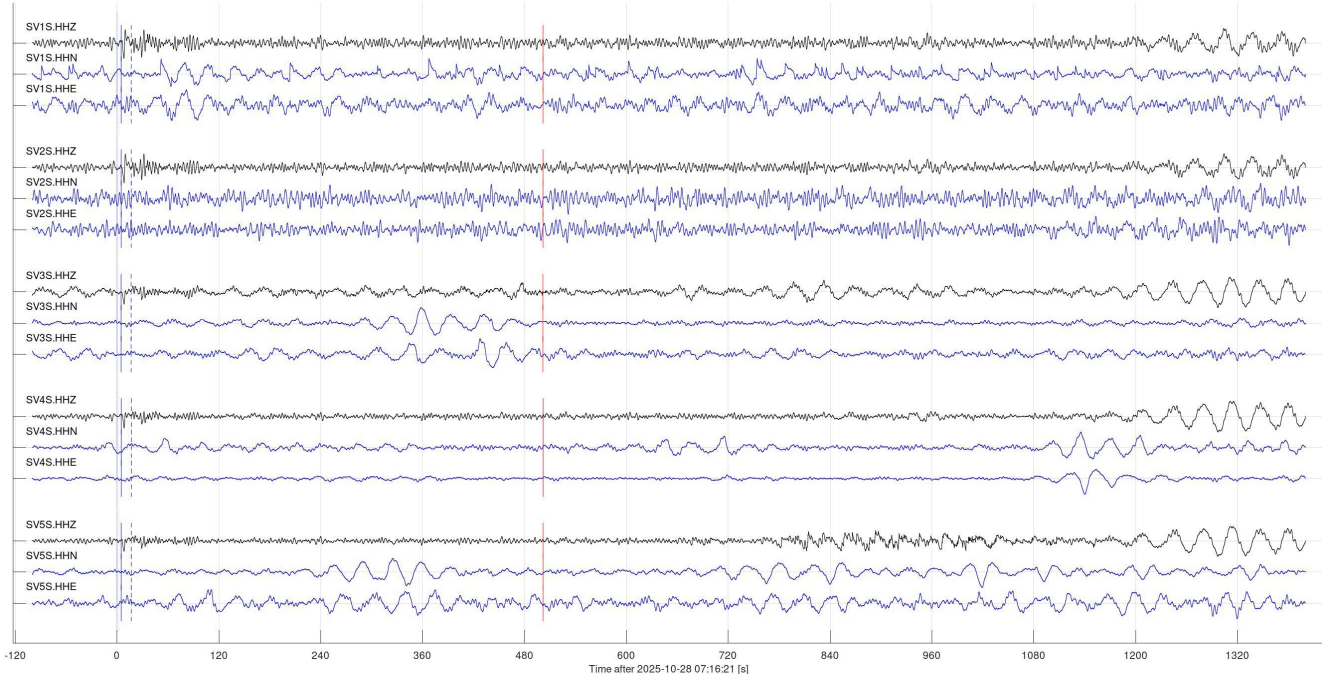


Figure 6, continued.

Event 32302 (us6000rjsu, us): mww 6.0; 2025-10-27 19:48:29 39.23N,28.23E: 4 km ESE of Sindirgi, Turkey
 $V_p=10.00$ km/s; $V_s=5.77$ km/s; $\text{baz}=36.1$ deg; $\text{dist}=82.1$ deg; $\text{depth}=8.00$ km

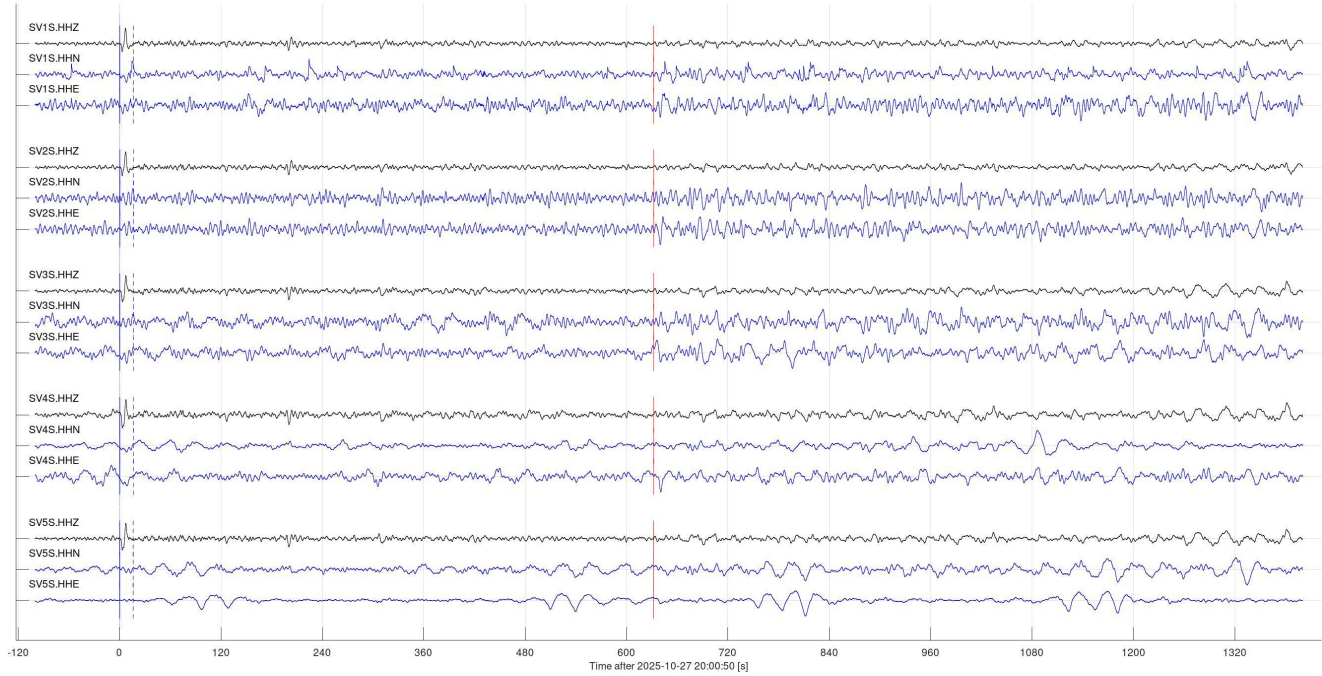


Figure 6, continued.

Event 32307 (us6000rjqj, us): mb 6.0; 2025-10-27 12:54:59 16.56N,59.56W: 163 km E of Beauséjour, Guadeloupe
 $V_p=10.00$ km/s; $V_s=5.77$ km/s; $\text{baz}=117.1$ deg; $\text{dist}=47.9$ deg; depth=10 km

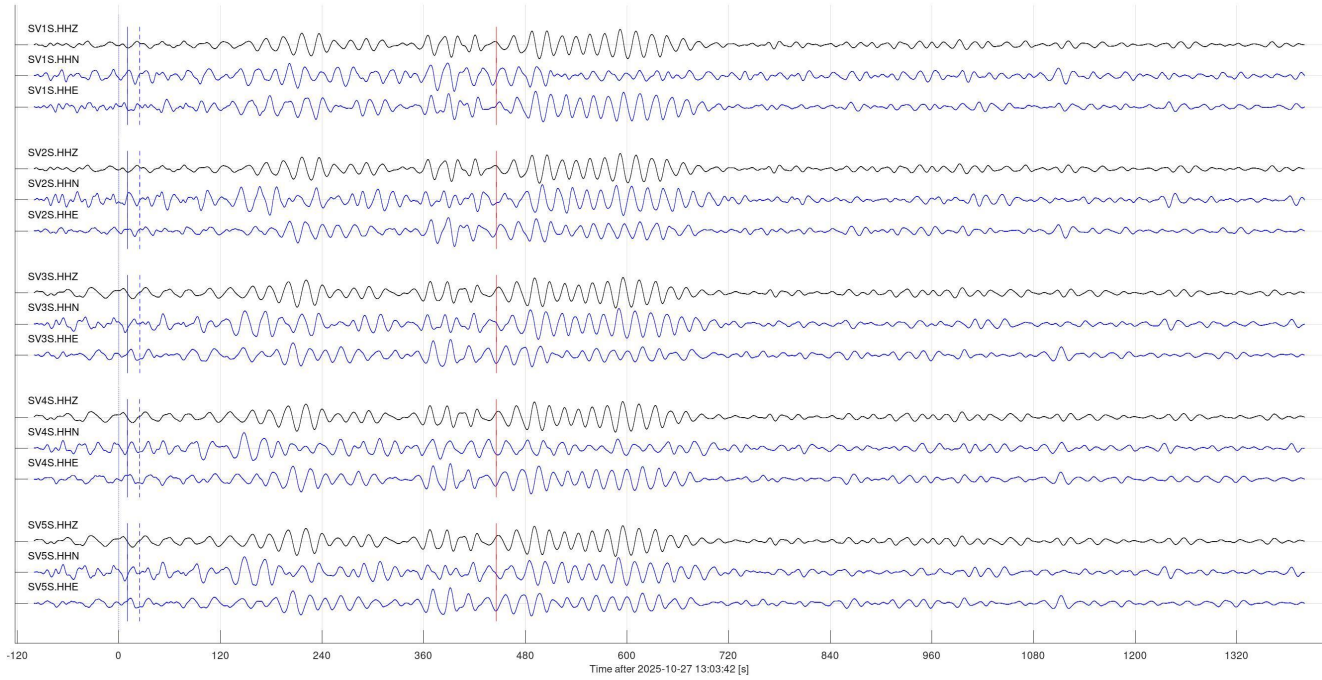


Figure 6, continued.

Event 32308 (us6000rjq8, us): mww 6.5; 2025-10-27 12:38:40 16.53N,59.57W: 162 km E of Beauséjour, Guadeloupe
 $V_p=10.00$ km/s; $V_s=5.77$ km/s; $\text{baz}=117.1$ deg; $\text{dist}=47.9$ deg; depth=9.00 km

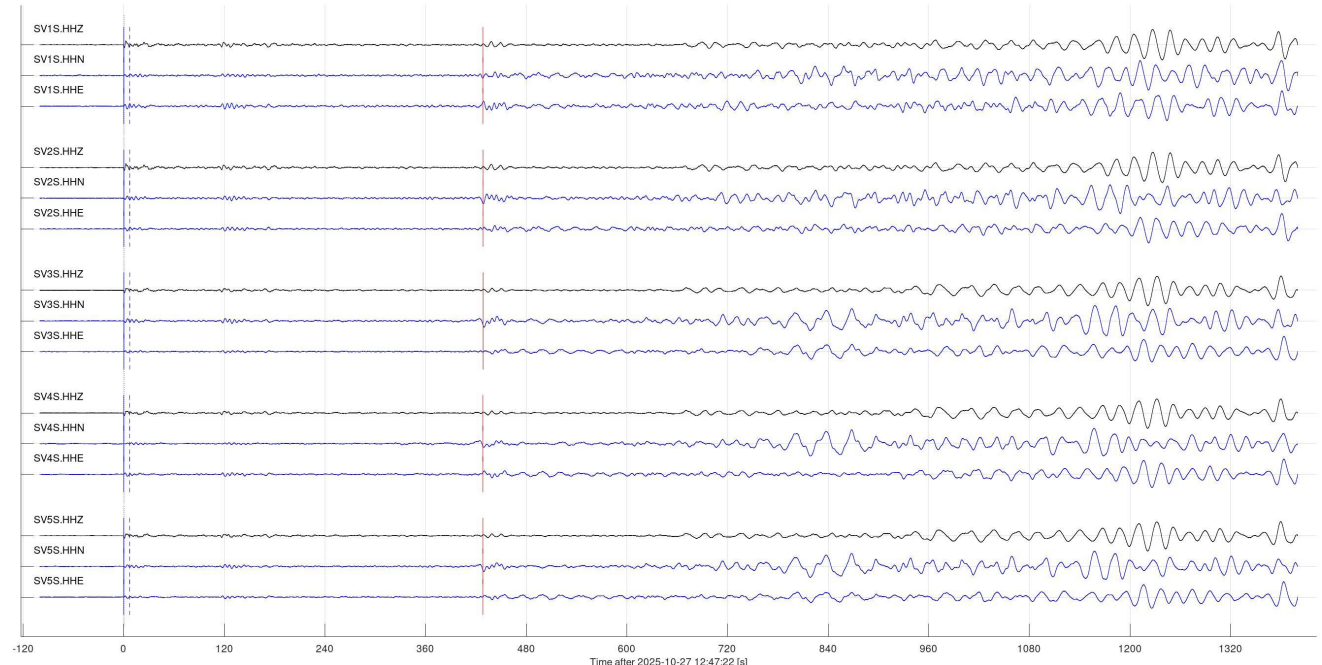


Figure 6, continued.

Event 32351 (us6000rjx3, us): mww 6.4; 2025-10-28 14:40:18 6.74S,130.02E: Banda Sea
 Vp=10.00 km/s; Vs=5.77 km/s; baz=295.1 deg; dist=118.7 deg; depth=142 km

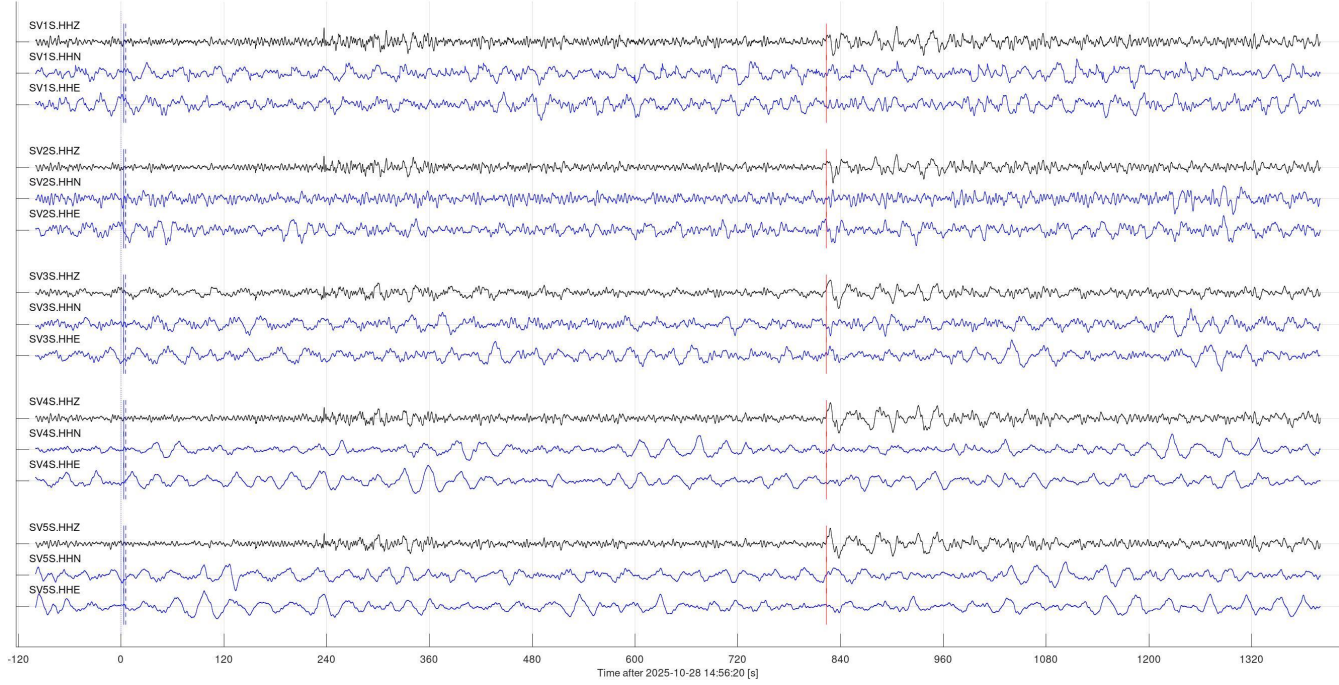


Figure 6, continued.

Event 32390 (us6000rk65, us): mww 5.4; 2025-10-29 16:46:30 64.74N,17.09W: 105 km WNW of Höfn, Iceland
 Vp=10.00 km/s; Vs=5.77 km/s; baz=36.8 deg; dist=45.5 deg; depth=10 km

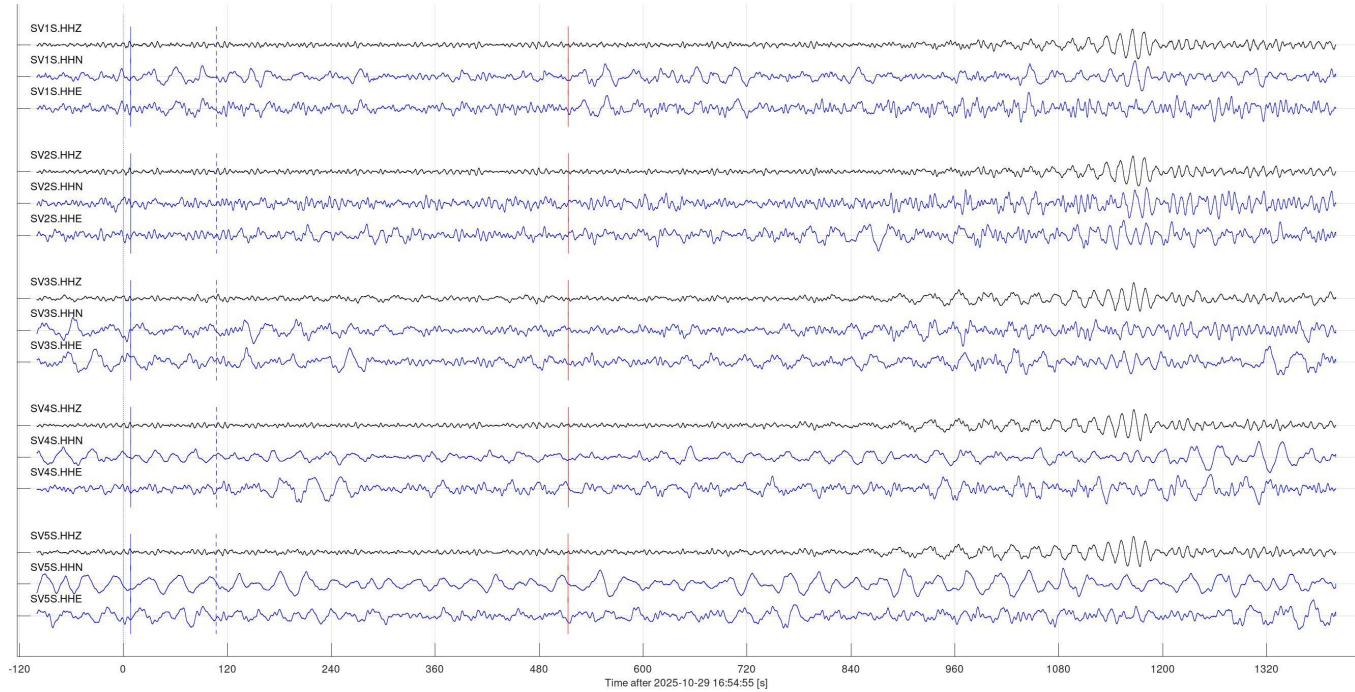


Figure 6, continued.

Event 32392 (us6000rk5r, us): mww 5.4; 2025-10-29 14:00:24 44.49N,129.54W: off the coast of Oregon
 $V_p=10.00$ km/s; $V_s=5.77$ km/s; $\text{baz}=265.7$ deg; $\text{dist}=18.7$ deg; depth=10 km

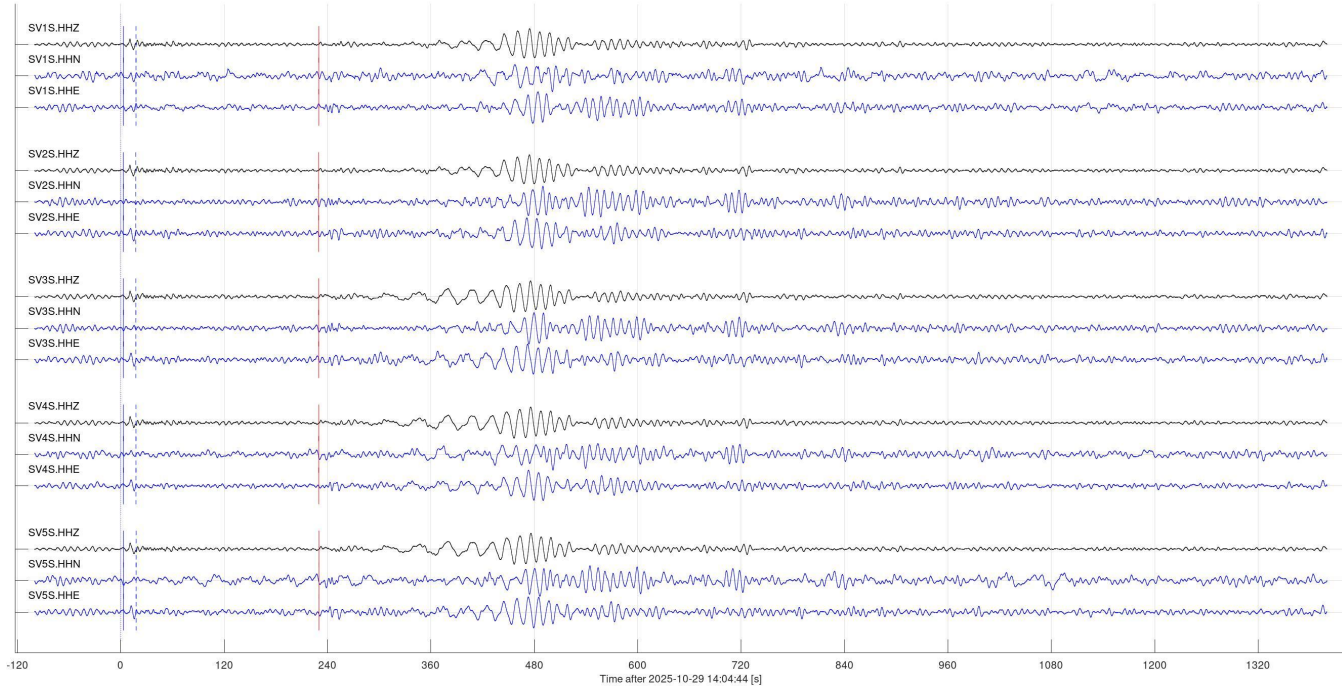


Figure 6, continued.

Event 32393 (us6000rk5p, us): mww 4.8; 2025-10-29 13:42:45 44.60N,129.82W: off the coast of Oregon
 $V_p=10.00$ km/s; $V_s=5.77$ km/s; $\text{baz}=266.3$ deg; $\text{dist}=18.8$ deg; depth=10 km

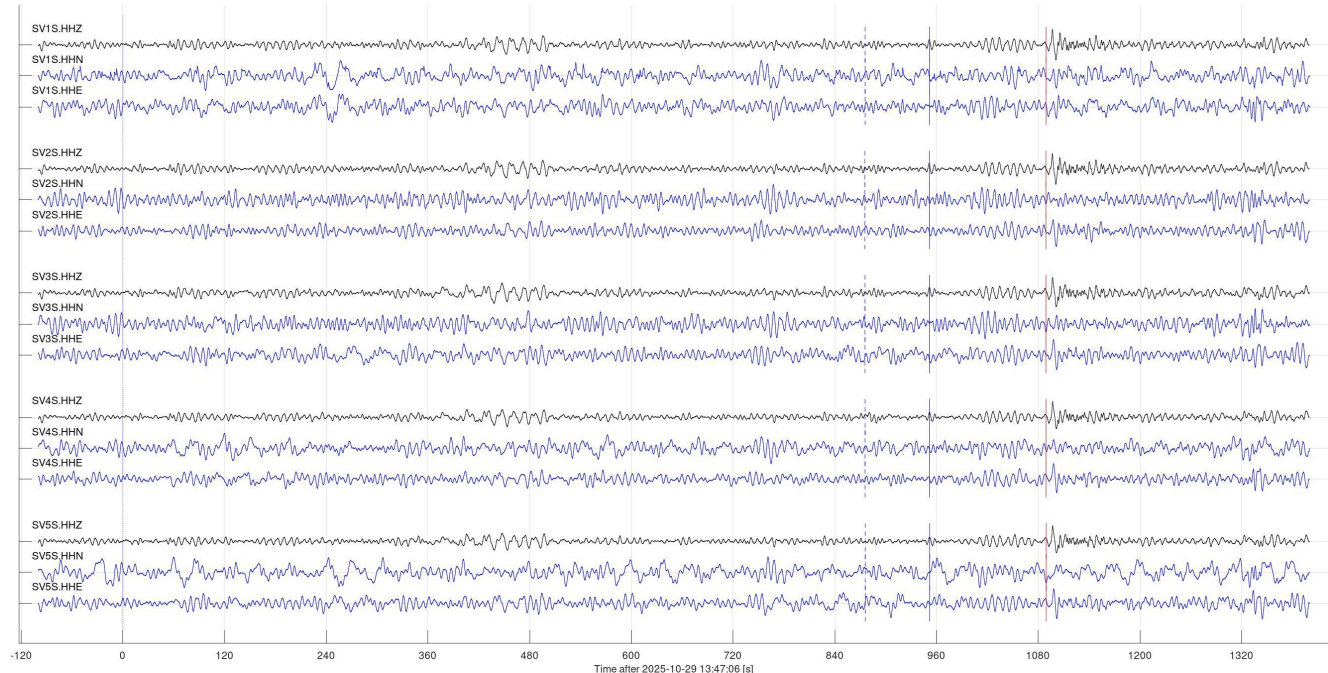


Figure 6, continued.

Event 32438 (ak025dxe5mlz, ak): ml 5.4; 2025-10-30 17:33:15 59.63N,150.23W: 48 km ESE of Fox River, Alaska
 $V_p=10.00$ km/s; $V_s=5.77$ km/s; $\text{baz}=309.4$ deg; $\text{dist}=28.8$ deg; depth=24 km

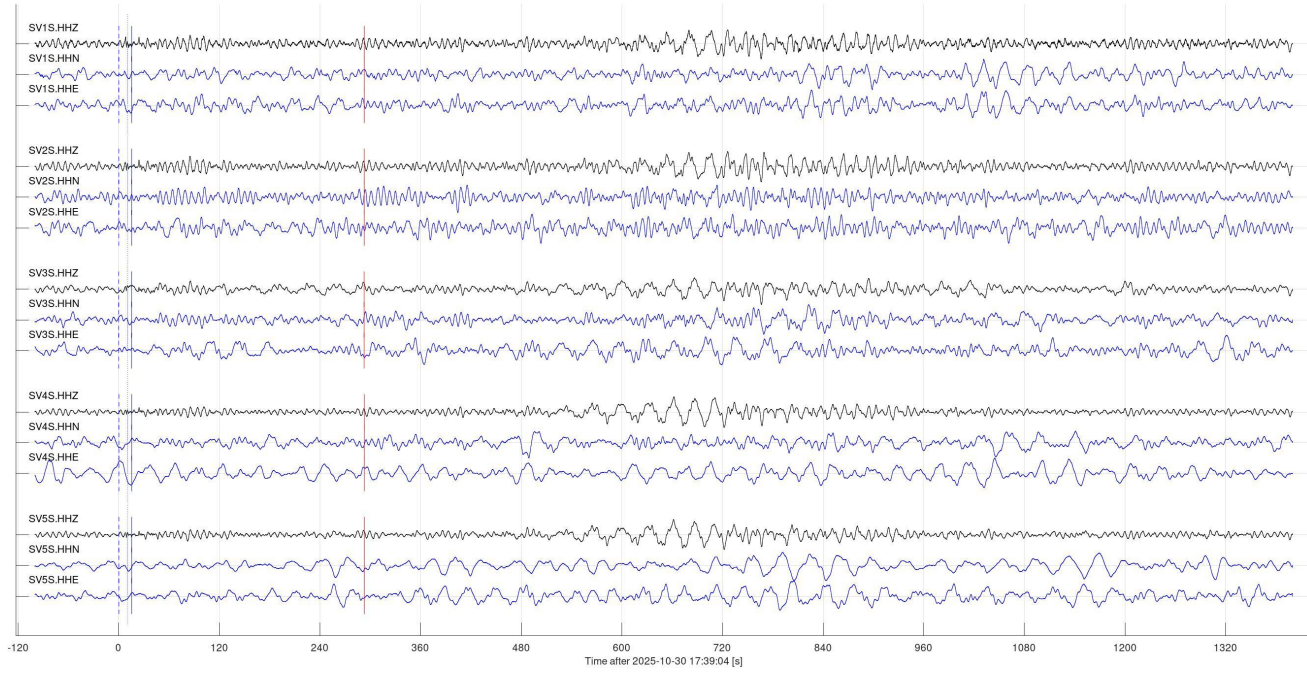


Figure 6, continued.

Regional events (class 2)

One regional seismic events (class 2 in Table 2) from Esterhazy, SK area was identified in the reporting period. This event was listed in the NRCan bulletin (Figure 5).

Event 34373 at 2025-10-13 05:07:18, 'Regional': mb 3.77 mining event 6 km ENE of Esterhazy, SK
 $V_p=6.20$ km/s; $V_s=3.50$ km/s; baz=90.0 deg; dist=1.7 deg; depth=0.00 km

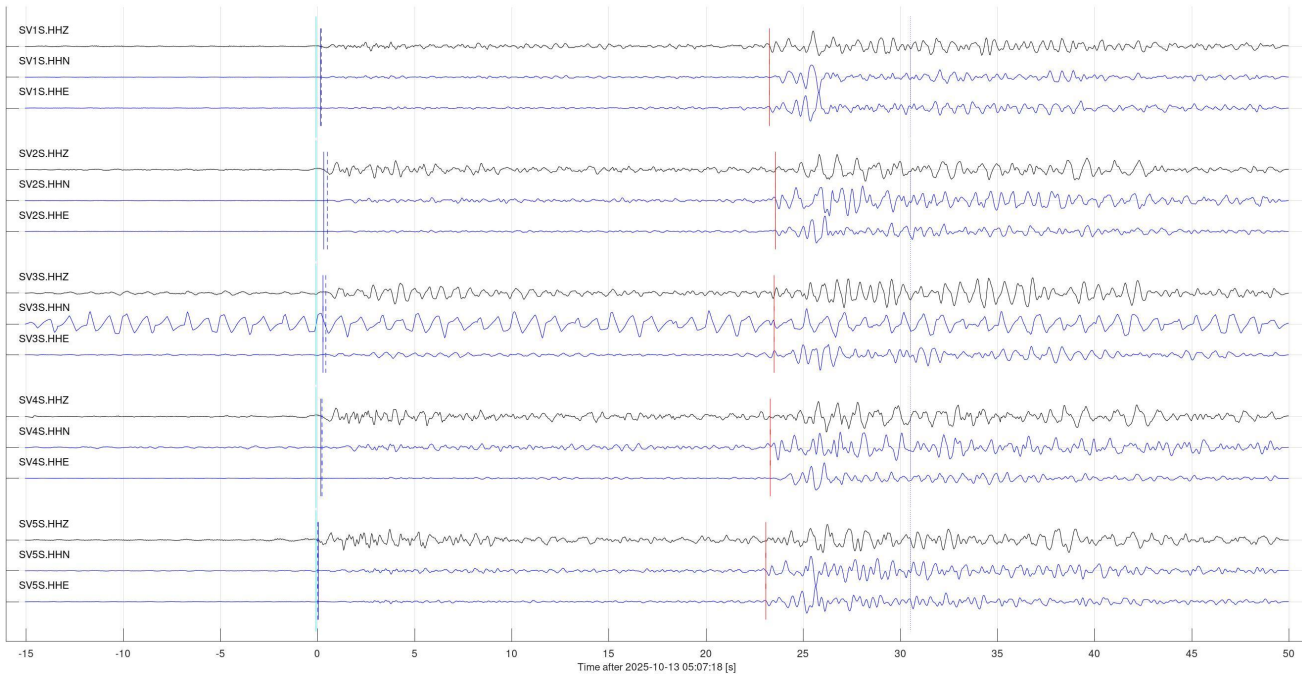


Figure 7. Regional seismic event near Esterhazy, SK.

Local events (classes 3 and 4)

The following subsections summarize observations of event classes 3 and 4 in Table 2.

Possible mine blasts at the Estevan mine (class 3a)

Ten detected events were identified as mine blasts in the area of Estevan coal mining (Figure 7). From these events, local P- and S-wave velocities, distances, and back-azimuths were roughly estimated. More accurate location work is in progress.

Event 35173 at 2025-10-02 21:40:36, 'Local': Possible mine blast near Estevan, SK
 $V_p=5.40 \text{ km/s}$; $V_s=2.80 \text{ km/s}$; $\text{baz}=90.0 \text{ deg}$; $\text{dist}=12.0 \text{ km}$; $\text{depth}=0.00 \text{ km}$

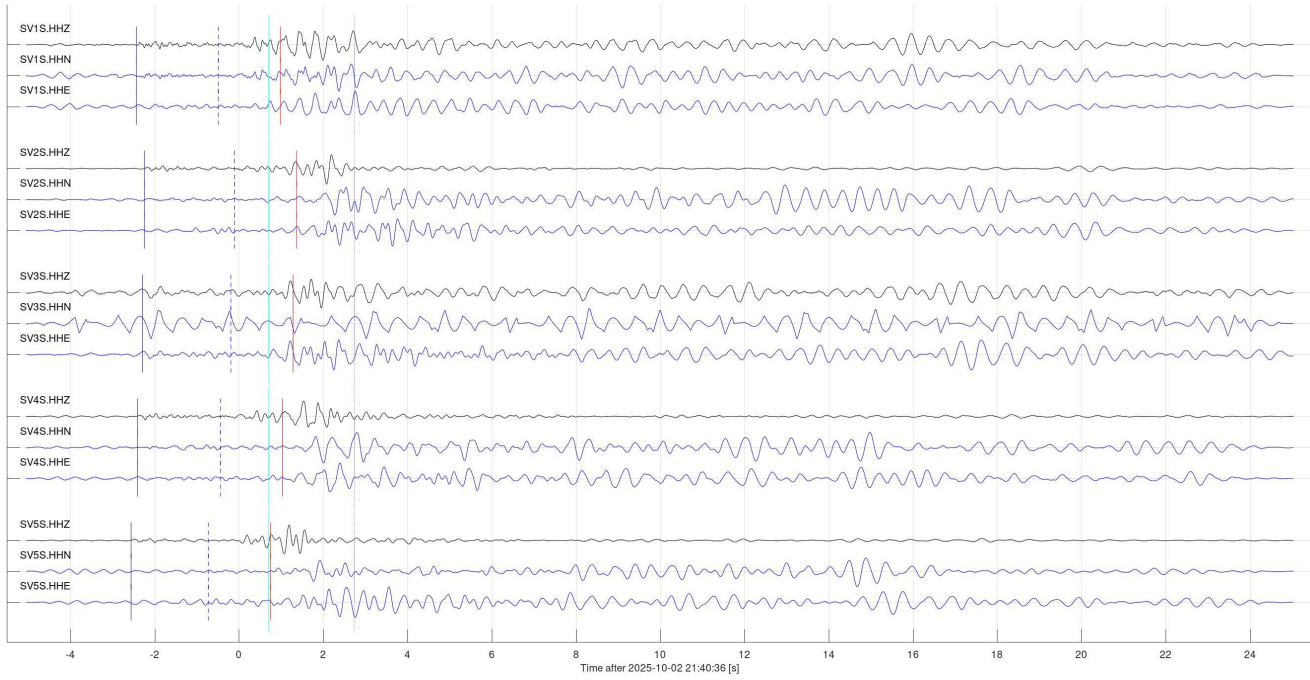


Figure 7. Seismic arrivals produced by mine blasts at the Estevan mine. Colours and labels are as in Figure 6.

Event 35176 at 2025-10-03 20:33:59, 'Local': Possible mine blast near Estevan, SK
 $V_p=5.40 \text{ km/s}$; $V_s=2.80 \text{ km/s}$; $\text{baz}=90.0 \text{ deg}$; $\text{dist}=12.0 \text{ km}$; $\text{depth}=0.00 \text{ km}$

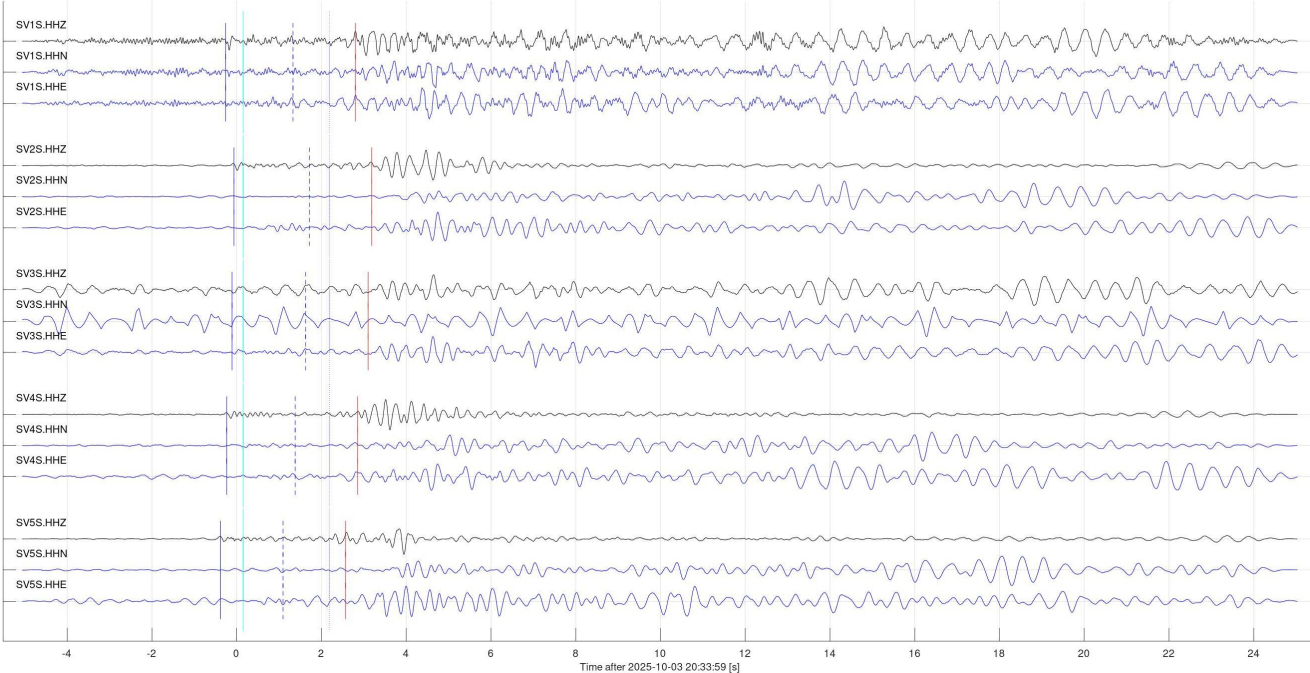


Figure 7, continued.

Event 35178 at 2025-10-04 21:09:16, 'Local': Possible mine blast near Estevan, SK
 $V_p=5.40$ km/s; $V_s=2.80$ km/s; $\text{baz}=90.0$ deg; $\text{dist}=12.0$ km; depth=0.00 km

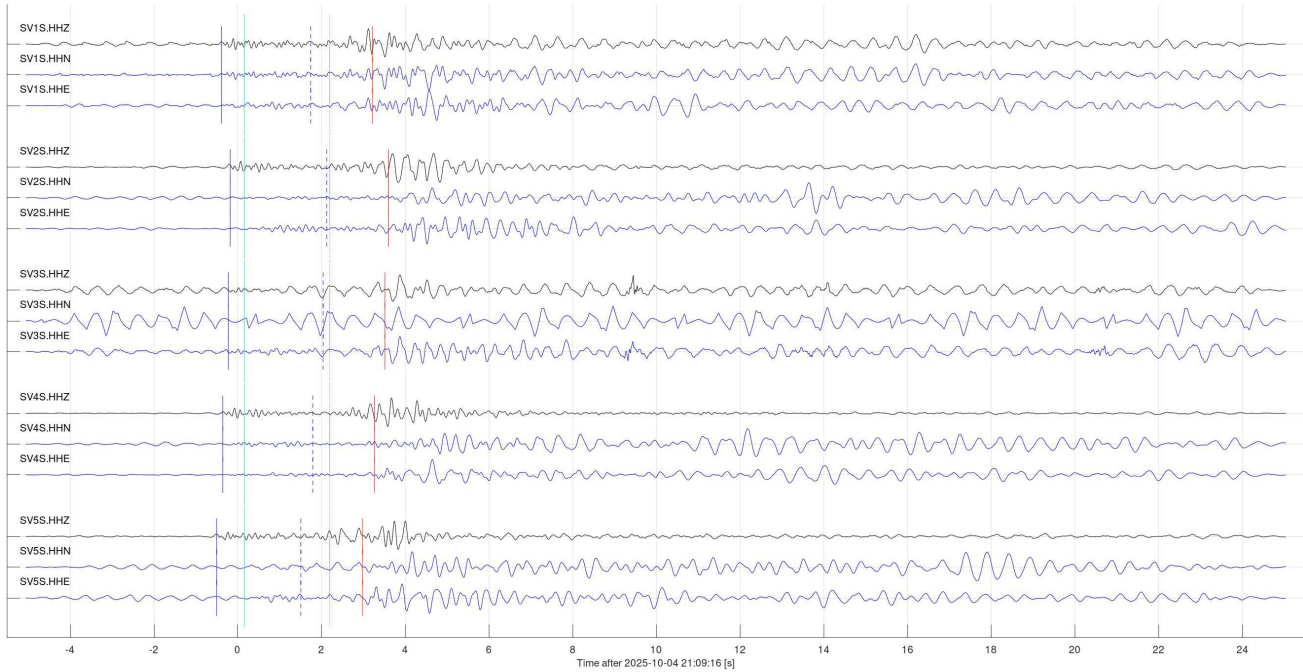


Figure 7, continued.

Event 35179 at 2025-10-05 21:29:25, 'Local': Possible mine blast near Estevan, SK
 $V_p=5.40$ km/s; $V_s=2.80$ km/s; $\text{baz}=90.0$ deg; $\text{dist}=12.0$ km; depth=0.00 km

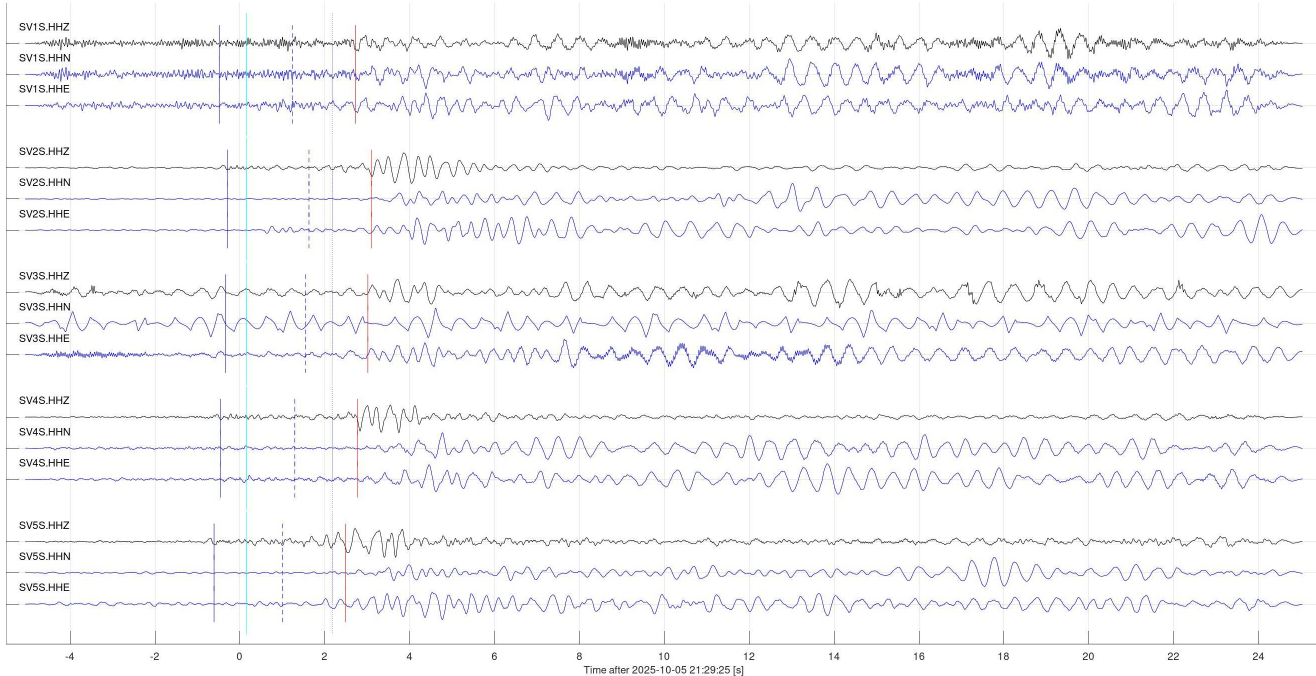


Figure 7, continued.

Event 35180 at 2025-10-06 21:14:41, 'Local': Possible mine blast near Estevan, SK
 $V_p=5.40$ km/s; $V_s=2.80$ km/s; $\text{baz}=90.0$ deg; $\text{dist}=12.0$ km; $\text{depth}=0.00$ km

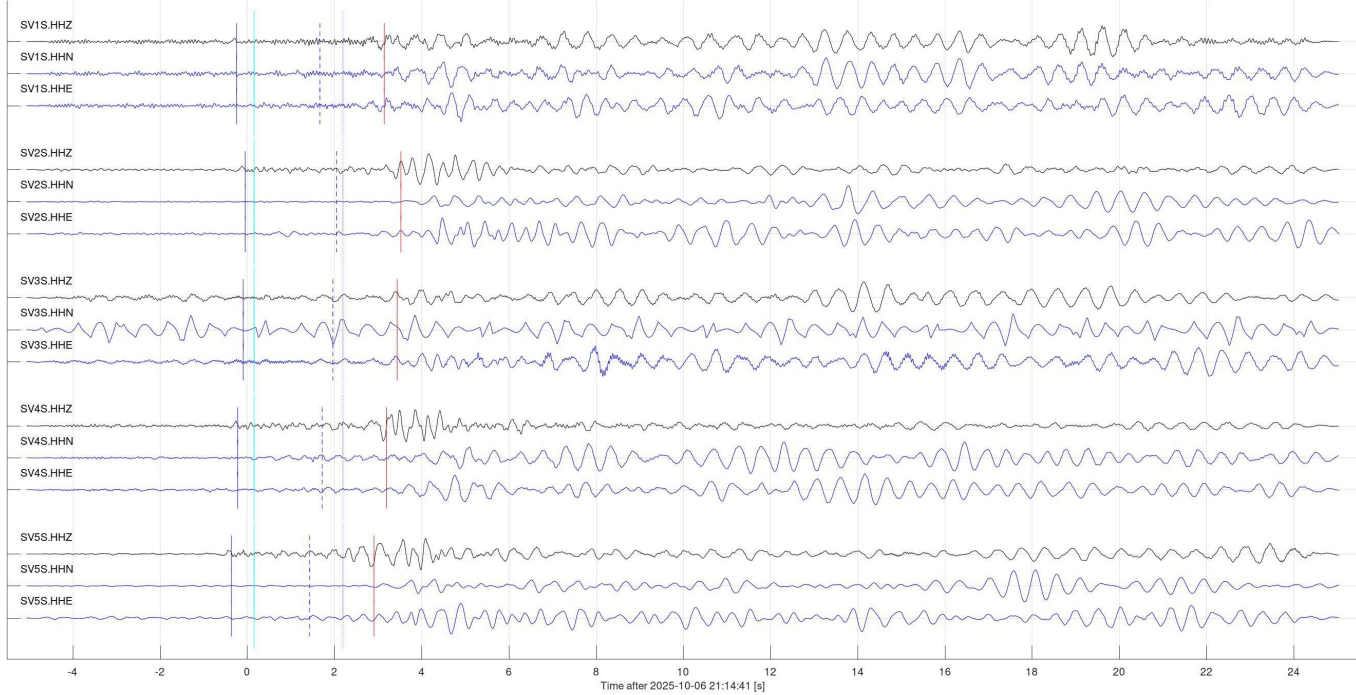


Figure 7, continued.

Event 35182 at 2025-10-07 21:22:36, 'Local': Possible mine blast near Estevan, SK
 $V_p=5.40$ km/s; $V_s=2.80$ km/s; $\text{baz}=90.0$ deg; $\text{dist}=12.0$ km; $\text{depth}=0.00$ km

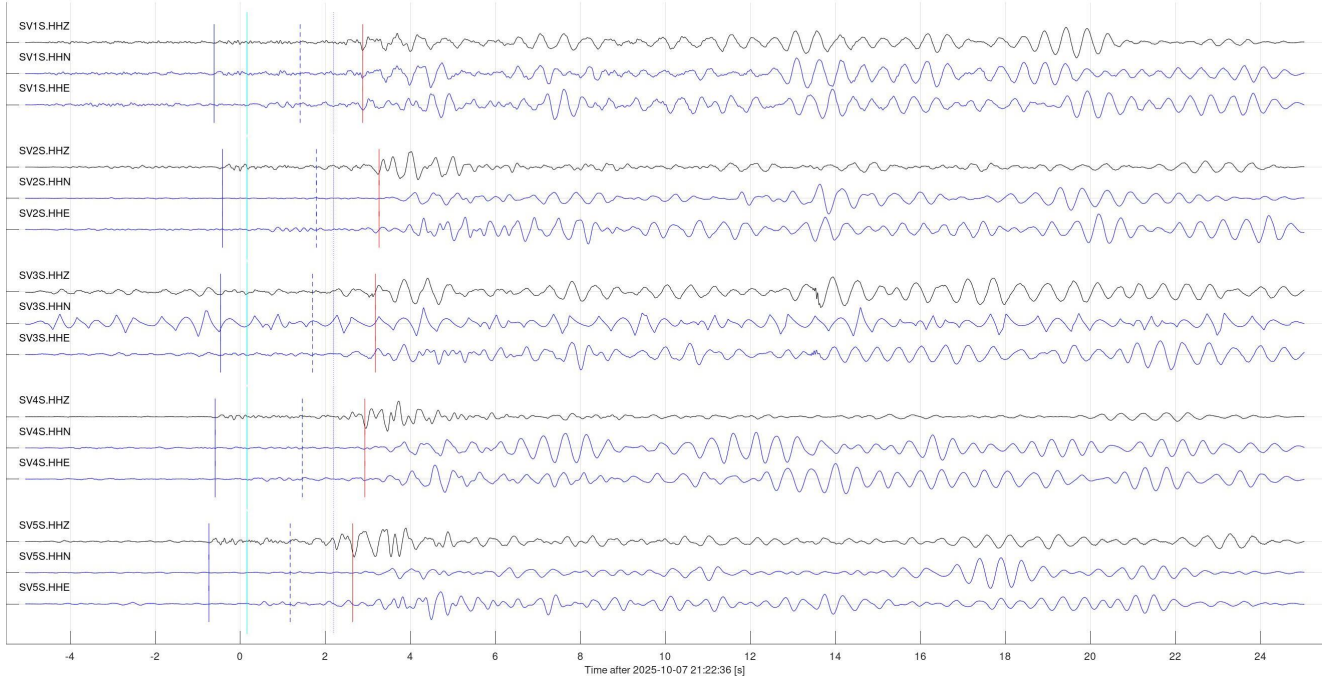


Figure 7, continued.

Event 35183 at 2025-10-10 20:08:43, 'Local': Possible mine blast near Estevan, SK
 $V_p=5.40$ km/s; $V_s=2.80$ km/s; $\text{baz}=90.0$ deg; $\text{dist}=12.0$ km; $\text{depth}=0.00$ km

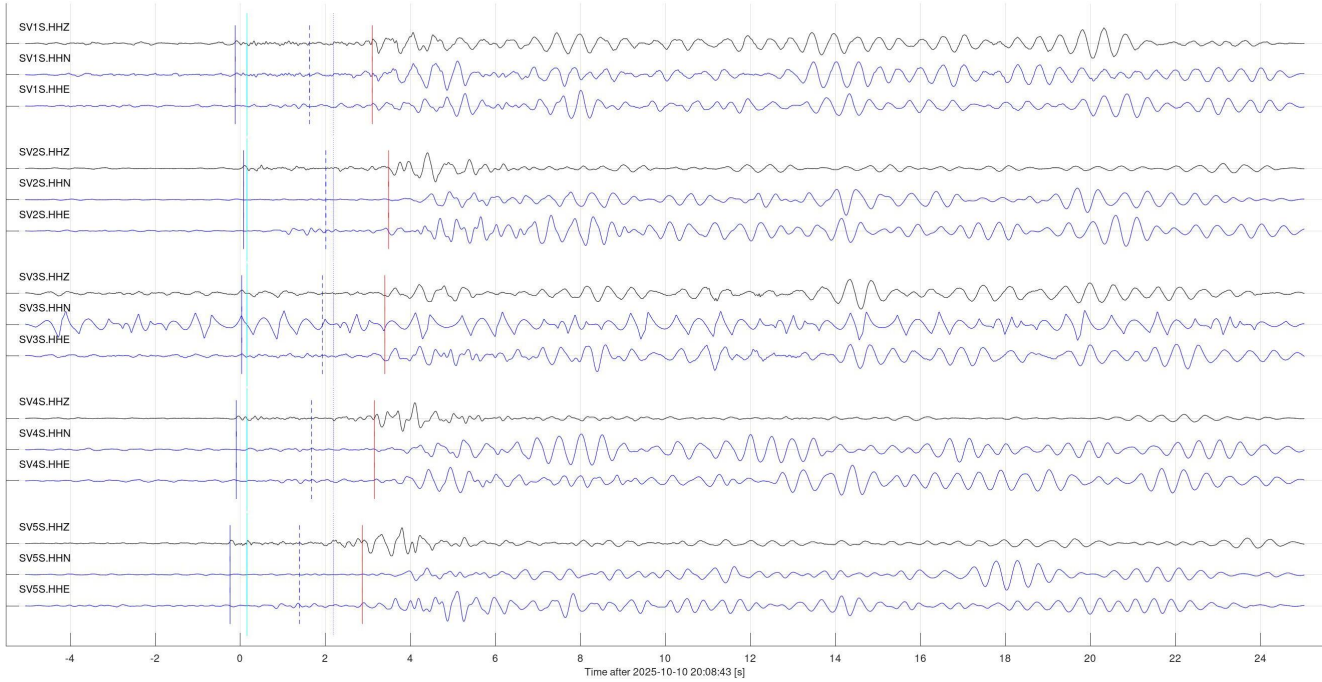


Figure 7, continued.

Event 35185 at 2025-10-28 21:55:46, 'Local': Possible mine blast near Estevan, SK
 $V_p=5.40$ km/s; $V_s=2.80$ km/s; $\text{baz}=90.0$ deg; $\text{dist}=12.0$ km; $\text{depth}=0.00$ km

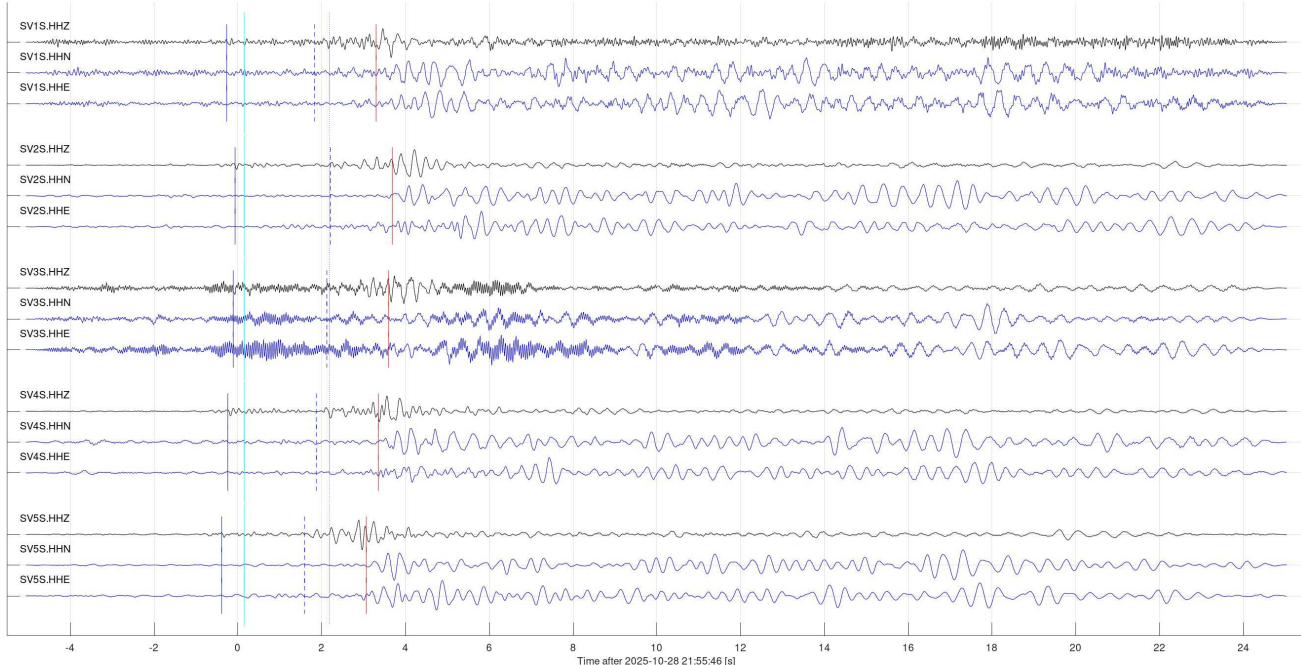


Figure 7, continued.

Event 35186 at 2025-10-30 21:40:16, 'Local': Possible mine blast near Estevan, SK
 $V_p=5.40 \text{ km/s}$; $V_s=2.80 \text{ km/s}$; $\text{baz}=90.0 \text{ deg}$; $\text{dist}=12.0 \text{ km}$; $\text{depth}=0.00 \text{ km}$

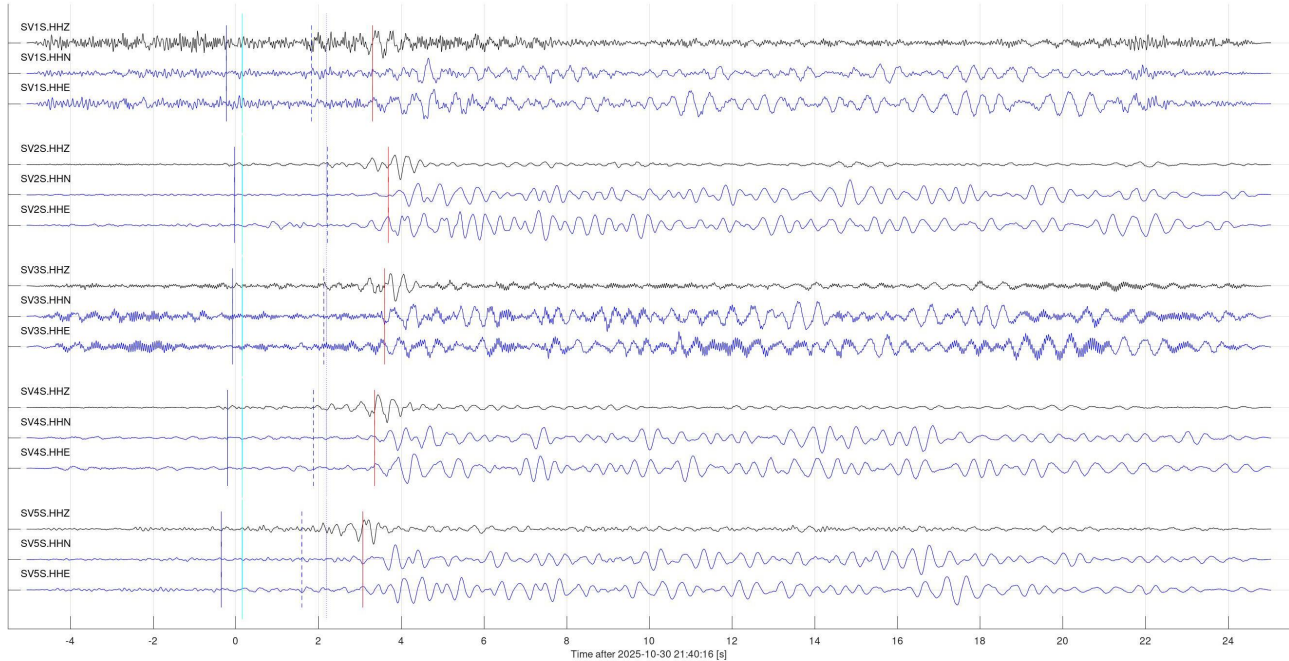


Figure 7, continued.

Event 35188 at 2025-10-31 21:30:24, 'Local': Possible mine blast near Estevan, SK
 $V_p=5.40 \text{ km/s}$; $V_s=2.80 \text{ km/s}$; $\text{baz}=90.0 \text{ deg}$; $\text{dist}=12.0 \text{ km}$; $\text{depth}=0.00 \text{ km}$

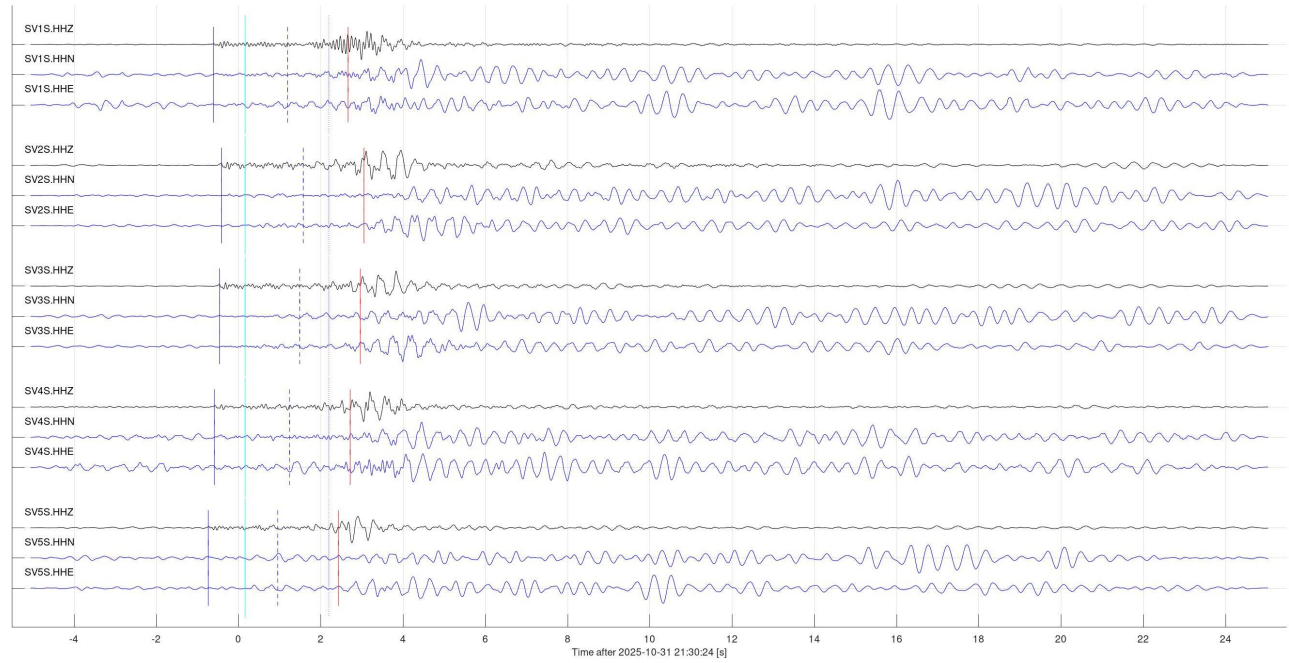


Figure 7, continued.

Events related to mining operations (class 3b)

Numerous mining- and industrial-operations related seismic events were observed in the area. To keep this report shorter, Figure 8 illustrates six of them, arbitrarily selected as appearing worth further analysis. Some of them (longer waveforms with strongly pronounced and lower dominant frequencies) may be produced by trains.

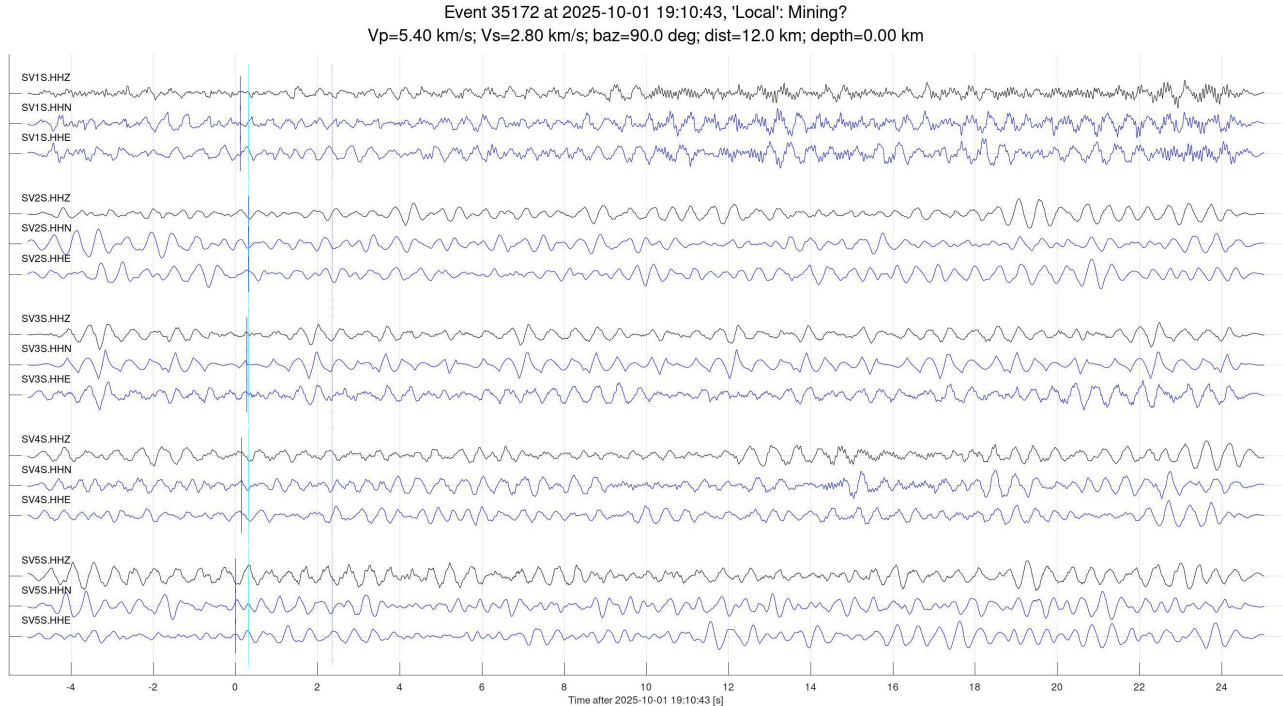


Figure 8. Sample events interpreted as due to mining activity in the area. Lines, colour bars and labels are as in the preceding figures.

Event 35174 at 2025-10-02 21:40:36, 'Local': Possible mine blast near Estevan, SK
 $V_p=5.40 \text{ km/s}$; $V_s=2.80 \text{ km/s}$; $\text{baz}=90.0 \text{ deg}$; $\text{dist}=12.0 \text{ km}$; $\text{depth}=0.00 \text{ km}$

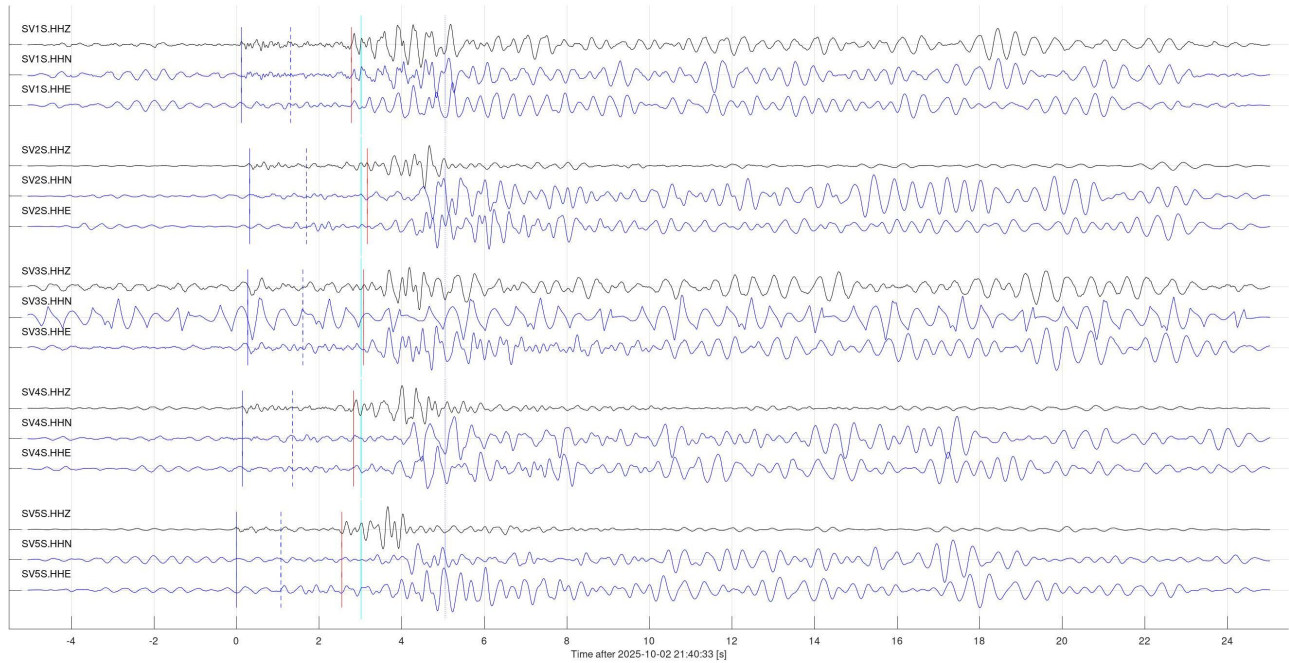


Figure 8, continued.

Event 35177 at 2025-10-04 20:51:11, 'Local': Mining?
 $V_p=5.40 \text{ km/s}$; $V_s=2.80 \text{ km/s}$; $\text{baz}=90.0 \text{ deg}$; $\text{dist}=12.0 \text{ km}$; $\text{depth}=0.00 \text{ km}$

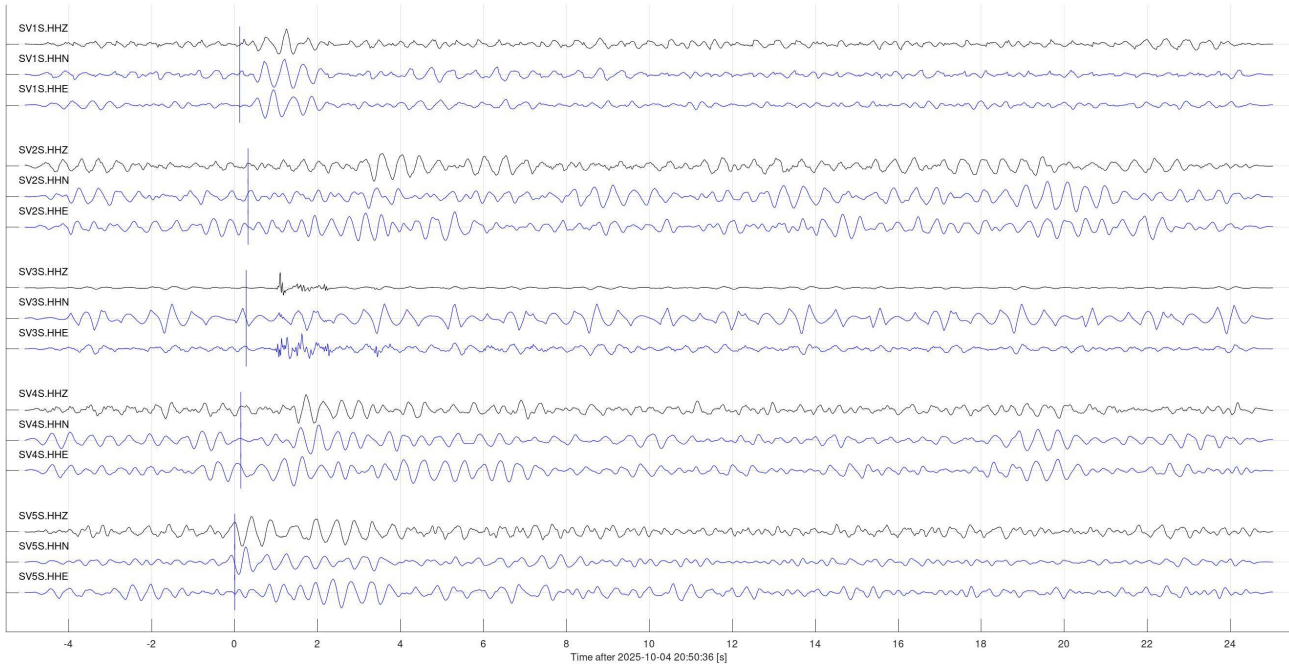


Figure 8, continued.

Event 35181 at 2025-10-07 20:50:23, 'Local': Mining?
 $V_p=5.40$ km/s; $V_s=2.80$ km/s; $\text{baz}=90.0$ deg; $\text{dist}=12.0$ km; depth=0.00 km

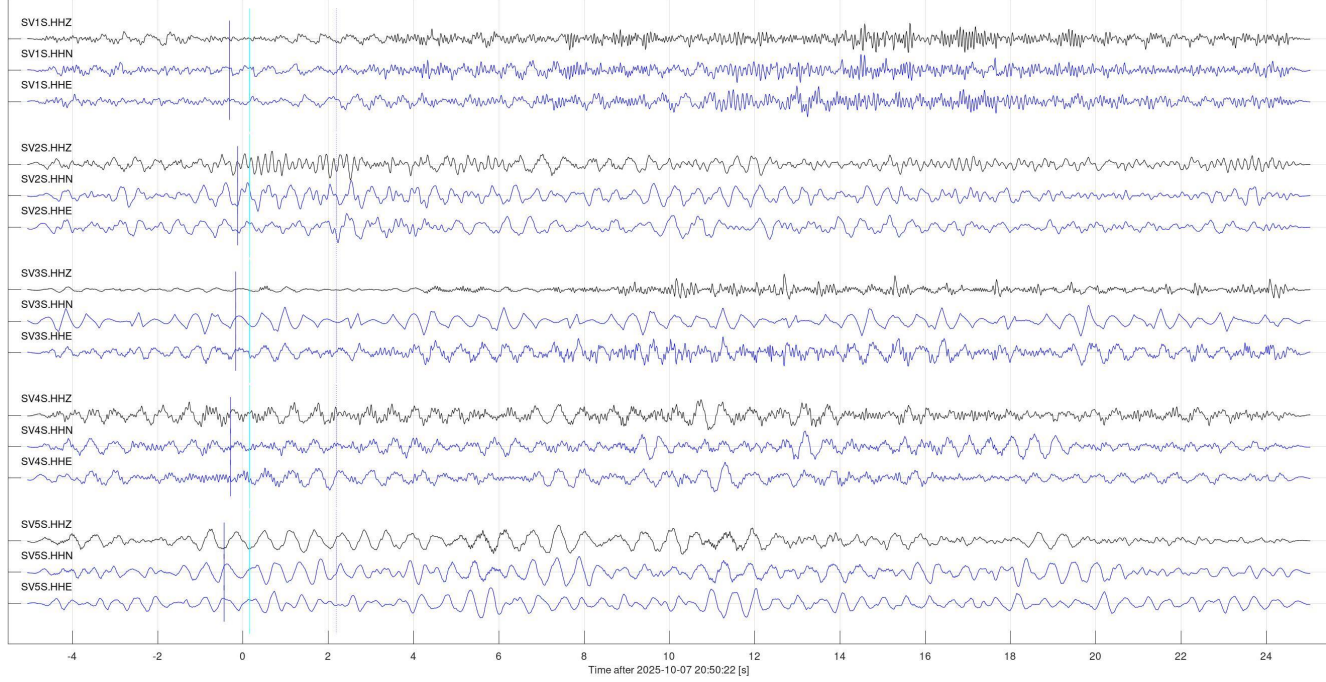


Figure 8, continued.

Event 35184 at 2025-10-13 22:33:02, 'Local': Mining?
 $V_p=5.40$ km/s; $V_s=2.80$ km/s; $\text{baz}=90.0$ deg; $\text{dist}=12.0$ km; depth=0.00 km

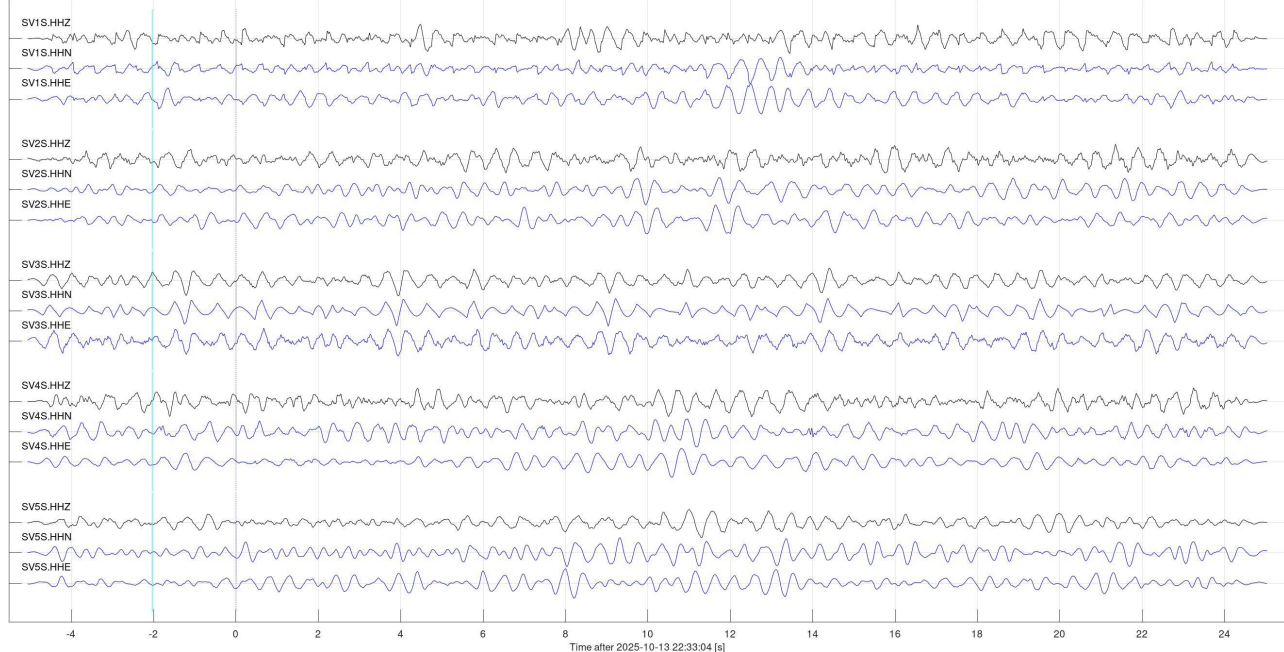


Figure 8, continued.

Event 35187 at 2025-10-31 20:40:53, 'Local': Mining?
 $V_p=5.40 \text{ km/s}$; $V_s=2.80 \text{ km/s}$; $\text{baz}=90.0 \text{ deg}$; $\text{dist}=12.0 \text{ km}$; $\text{depth}=0.00 \text{ km}$

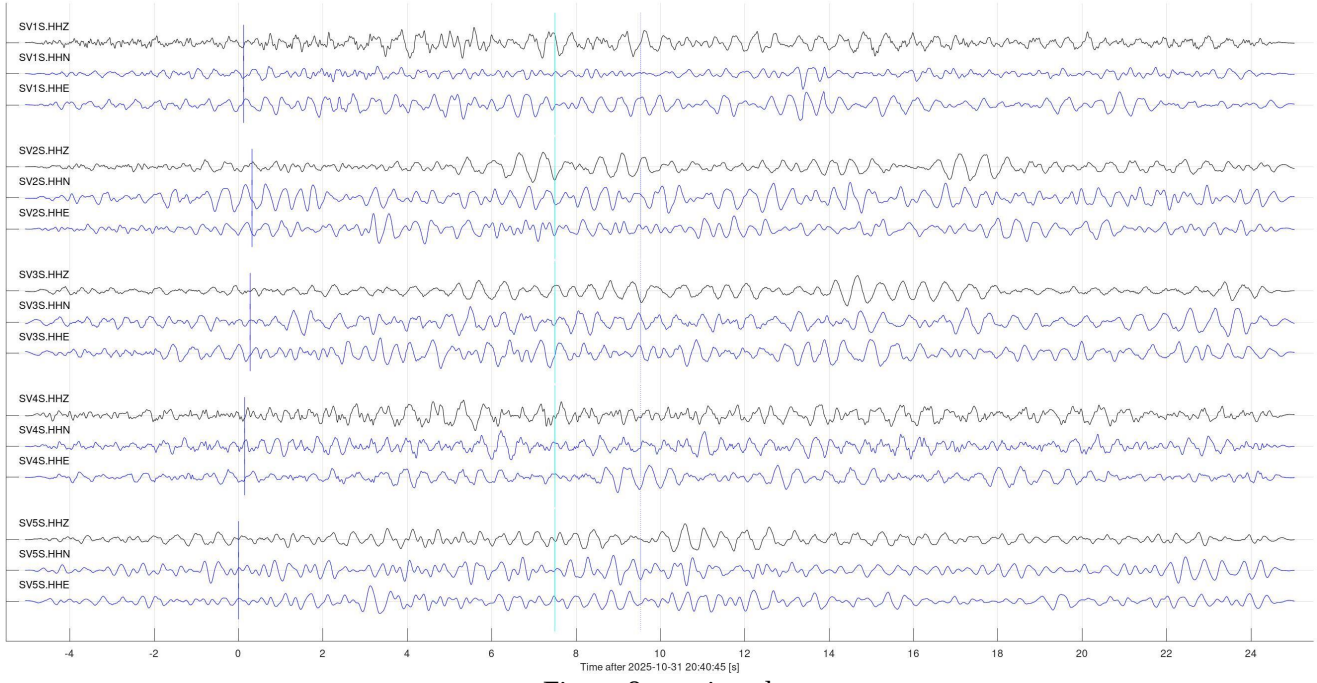


Figure 8, continued.

Events in array proximity (classes 4a and 4b)

One seismic event was identified as possibly occurring in the proximity of the array (class 4a) (Figure 9). All similar events I have seen so far likely originate in the near surface, as indicated by strong differences in frequency content and large travel-time moveouts.

Event 35175 at 2025-10-02 22:46:09, 'Near': Near SV5S?
 $V_p=2.40 \text{ km/s}$; $V_s=1.20 \text{ km/s}$; $\text{baz}=90.0 \text{ deg}$; $\text{dist}=1.0 \text{ km}$; $\text{depth}=0.00 \text{ km}$

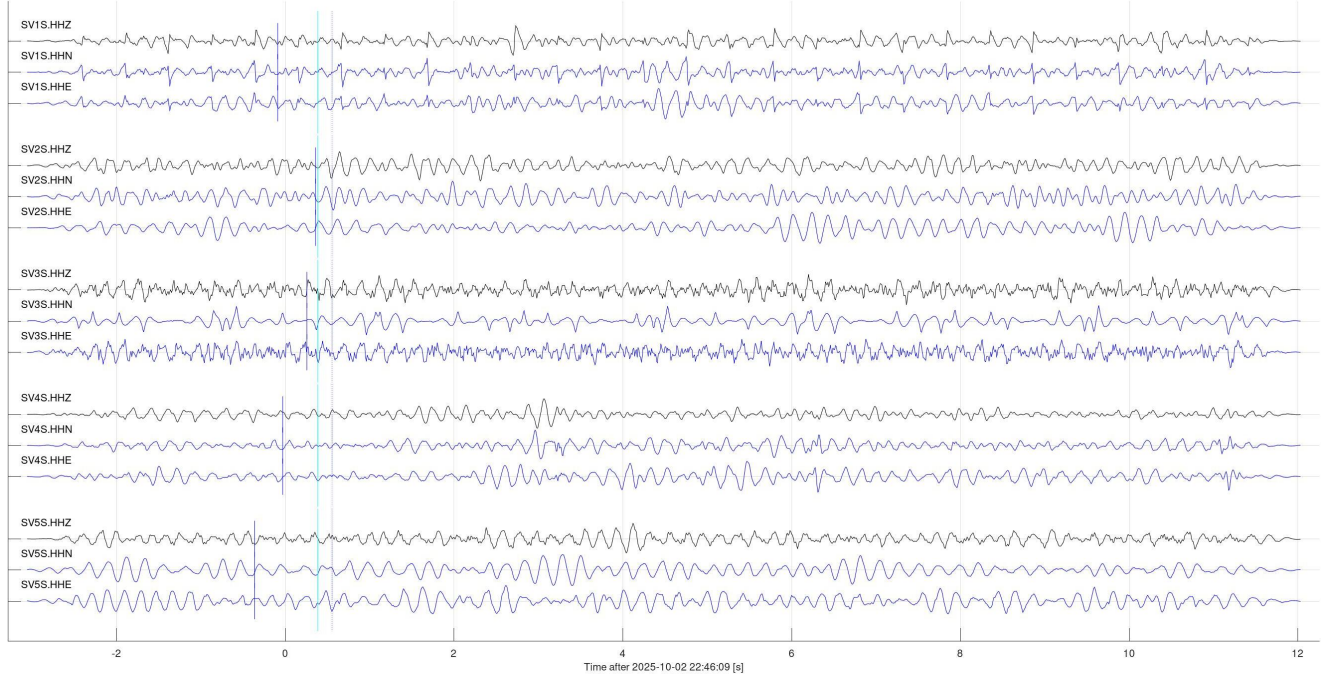


Figure 9. Event interpreted as occurring near surface in the proximity of the array (class 4a in Table 2). Lines, colour bars and labels are as in the preceding figures. Seismic velocity estimates shown in the headers (particularly P-wave) are from an averaged model and require further analysis.

5. SEGY files

Event time windows are provided in SEGY format in the attached zipped archive, separately for teleseismic and regional event detections. Subdirectory names and file naming convention and header formats are described in our reports for August and October 2024.

6. Conclusions and recommendations

Conclusions and recommendations are close to the preceding report:

- The Aquistore is currently in good condition, with nearly 100% data recovery and only one horizontal-component channel SV5S.HHE faulty.
- Thirty strong teleseismic events and ten mine blasts were detected in October 2025.

- Numerous local events were detected, likely related to mining operations or freight trains. These events were not catalogued or analyzed in detail.
- One event potentially occurring near-surface in the vicinity of the array was noted. Such events are extremely difficult to differentiate from industrial noise in the area. No events occurring at the reservoir level were identified.